COMPARISON OF DEFLECTION MEASUREMENT METHODS OF LARGE DIAMETER STEEL PIPES WITH CONTROL LOW STRENGTH MATERIAL

by

SAMAN FARROKHI GOZARCHI

Presented to the Faculty of the Graduate School of

The University of Texas at Arlington in Partial Fulfillment

of the Requirements

for the Degree of

MASTER OF SCIENCE IN CIVIL ENGINEERING

THE UNIVERSITY OF TEXAS AT ARLINGTON

August 2014

Copyright © by Saman Farrokhi Gozarchi 2014

All Rights Reserved

Acknowledgements

I would like to thank my research advisor Dr. Ali Abolmaali for giving me the opportunity to work under his supervision at the UT Arlington Center for Structural Engineering Research (UT Arlington-CSER). For his endless support and guidance I am forever grateful. I would like to also acknowledge the other members of my committee, Dr. Siamak Ardekani and Dr. Yeonho Park for their keen advice and review of my research and for their constant support throughout my academic career.

I am grateful to the entire group of CSER fellow researchers for their help in volunteering with field measurements, with special thanks to Margarita Takou for her constant support and guidance. In addition I would also like to thank Dr. Yeonho Park the experimental program director at CSER and Dr. Mohammad Razavi and Dr. Mojtaba Dezfooli for their expert guidance and for coordinating the field measurements. I would also like to thank Kahle Loveless the project administrator at Garney Construction for his tremendous effort, time, resources and guidance in helping with this research.

Finally I would like to thank my family for their endless support and encouragement to further my education.

May 12th, 2014

Abstract

COMPARISON OF DEFLECTION MEASUREMENT METHODS OF LARGE DIAMETER STEEL PIPES WITH CONTROL LOW STRENGTH MATERIAL

Saman Farrokhi Gozarchi, M.S

The University of Texas at Arlington, 2014

Supervising Professor: Ali Abolmaali

This study investigates the structural integrity of large diameter (108 inch) steel pipes with mortar lining embedded with Controlled Low Strength Material (CLSM) during installation. Field tests were carried out in the prove-out section of line J which is a 2 mile (3.21 km) section of an Integrated Pipeline network (IPL) that will ultimately run a length of 150 mile (241.4 km) from Lake Palestine to Lake Benbrook. The prove-out is a section of line J that was used for experimental research for the use of CLSM as an embedment material and calibrate Finite Element Method (FEM) model for the rest of the pipeline. The prove-out section is comprised of 11 pipes, varying in length from 24 ft. to 50 ft. (7.3-15.2 m), with a total length of 518 ft. (157.8 m). The project integrates existing Tarrant Regional Water District (TRWD) pipelines to Dallas systems to provide 350 million gallons per day (1.32 Billion liters per day) of raw water supplies to more than 1.8 million people in 11 counties in North Texas.

Three methods were used to check for deflection measurements: Manuals and Reports on Engineering Practice No.119 (MOP-119) method, Laser Photo Profile and Laser Video Profile. The MOP-119 method is utilized from American Society of Civil Engineers (ASCE) Buried Flexible Steel Pipe (2009). The deflections of the steel pipes were effectively measured in each of the installation stages. The installation stages

considered for this research were pipe placement, CLSM embedment at 30% pipe diameter, CLSM embedment at 70% pipe diameter, and backfill with and without stulls. Forty-three (43) sections were measured using the MOP-119 and Laser Photo Profile methods (about 12 feet or 3.65 meters a section) per installation stage. The laser video profile method was run continuously on one site visit for the entire prove-out section. The MOP-119 method was compared to the Laser Photo Profile method while stulls were present in the pipeline and later with both the Laser Photo and Video Profile method when stulls were removed. For large diameter steel pipes with mortar lining the recommended limit for deflection is set at 2% of the pipes diameter according to American Water Works Association (AWWA M11).

Material tests were conducted in the Civil Engineering Laboratory Building (CELB) to check for flexural and compressive strength of CLSM based on ASTM C78/C78M-10 (Standard Test Method for Flexural Strength of Concrete) and ASTM D4832-10 (Standard Test Method for Preparation and Testing of CLSM Test Cylinders).

It was observed after processing the field measurement data that the MOP-119 method yielded a higher deflection limit than the Laser Photo Profile and Laser Video Profile methods which were within the deflection limit of two percent (2%) as per AWWA specification.

Table of Contents

Acknowledgements iii

Abstract iv

List of Illustrations viii

List of Tables xii

Chapter 1 Introduction, Literature review, Objective 1

1.1 Introduction 1

1.1.1 Pipe Mechanics and Installation 1

1.1.2 Pipe Design 10

1.1.3 Controlled Low Strength Material 16

1.2 Literature Review 20

1.3 Objective 25

1.3.1 Justification of Research 26

Chapter 2 Field Test 27

2.1 Introduction 27

2.2 MOP-119 Method 35

2.3 Laser Photo Profile Method 37

2.4 Laser Video Profile Method 42

2.5 Field Test Results 50

2.6 CLSM Material Testing 57

2.6.1 CLSM Casting 58

2.6.2 CLSM Testing 59

2.6.3 Results 62

Chapter 3 Summary, Conclusion and Recommendation 64

3.1 Summary 64

3.2 Conclusion 65

3.3 Recommendation 66

Appendix A MOP-119 method for middle ordinate values at 90 degrees 67

Appendix B MOP-119 method for middle ordinate values at 45 degrees 79

References 91

Biographical Information 94

List of Illustrations

Figure 1-1 Schematic of the typical terminologies used in pipe and trench configurations from ASCE Buried Flexible Steel Pipe (2009) 2
Figure 1-2 Steel trench shield to protect the trench walls from collapsing while excavating 5
Figure 1-3 Sandbag placement beneath pipe 5
Figure 1-4 Backfilling of prove-out section using native soil 6
Figure 1-5 Trench configuration used in the section J of IPL 7
Figure 1-6 Cross section view of bond between steel pipes and cement mortar 8
Figure 1-7 Wooden stull configurations (a) Vertical (b) Crossed (c) Three legs 9
Figure 1-8 Configuration of steel bracing (a) Vertical (b) Crossed 9
Figure 1-9 Types of cracks observed in prove out-section (a) Small longitudinal cracks (b) 1 inch crack (c) Circumferential crack 13
Figure 1-10 Maximum deflection estimation (a) Schematic location of middle ordinate (b) Relationship of ratio of radii to elliptical ring deflection courtesy of MOP-119 15
Figure 1-11 Schematic of symmetric and unsymmetrical deformations observed in pipeline 16
Figure 1-12 Comparison of maximum principal stresses between Granular soil with and without Portland cement from ASCE Buried Flexible Pipe (2009) 18
Figure 2-1 Aerial view of the prove-out section and site location 27
Figure 2-2 Schematic of installation phases (a) placement (b) CLSM embedment at 30% pipe diameter (c) CLSM embedment at 70% pipe diameter (d) backfill 28
Figure 2-3 Schematic of the 3 different pipe joint lengths and sections where measurements were taken (a) 50 ft. joint (b) 44 ft. joint (c) 24 ft. joint 31
Figure 2-4 Placement of pipeline within trench 32

Figure 2-5 Safety equipment and clothing required 33
Figure 2-6 Blower unit used in the prove-out section 33
Figure 2-7 30 in. manhole 34
Figure 2-8 Personnel and equipment entering manhole (a) equipment craned (b) personnel entering manhole via ladder (c) equipment lowered into manhole 34
Figure 2-9 Schematic of MOP-119 method for calculating radius of curvature of deformed pipe 35
Figure 2-10 Instrument configuration used to measure middle ordinate by MOP-119 method 36
Figure 2-11 Mop-119 measurements taken per section at (a) 90 degree (b) 45 degree . 37
Figure 2-12 Laser photo profile instrumentation (a) ten-head laser ring with rechargable battery on skid (b) high resolution camera on tripod (c) scale 38
Figure 2-13 Placement of skid along pipe axis symmetry and stability 39
Figure 2-14 Laser photo profile method at start of pipe joint number 1066 at placement 40
Figure 2-15 Laser photo profile method at 10ft of pipe joint number 1066 at placement . 40
Figure 2-16 Laser photo profile method at 25ft of pipe joint number 1066 at placement . 41
Figure 2-17 Laser photo profile method at 40ft of pipe joint number 1066 at placement . 41
Figure 2-18 Laser photo profile method at end of pipe joint number 1066 at placement . 42
Figure 2-19 Instrumentation for the laser video profile method (a) data logger and console (b) ten-head laser ring on skid (c) crawler with video camera (d) gas generator (e) cable extension 43
Figure 2-20 Movement of instrumentation for placement within the pipeline 44
Figure 2-21 Extension power lines (a) through inlet along pipeline (b) temporary power inlet hole 44

Figure 2-22 Set-up of data logger and console unit (a) data logger and console unit (b) Crawler camera and lighting control (c) Monitoring laser ring diameter from Inspector General display 45
Figure 2-23 Crawler and laser-skid placement (a) Crawler to data logger cable connection (b) Crawler to laser-skid cable connection (c) ten-head laser ring placement (d) Rechargeable battery connection and placement 46
Figure 2-24 Distance required between crawler and laser-skid 47
Figure 2-25 High resolution camera on crawler 47
Figure 2-26 Debris within pipeline (a) welding joint debris (b) installation debris 48
Figure 2-27 Crawler being pulled back by data logger and console connecting cable (a) data logger and console connecting cable (b) crawler pulled back 48
Figure 2-28 Pipe diameter check via rod (a) vertical deflection (b) horizontal deflection . 49
Figure 2-29 Pipe diameter check via laser distance meter (a) horizontal deflection (b) vertical deflection 50
Figure 2-30 Percent deflection obtained from the MOP-119 method for each section of installation phase 51
Figure 2-31 Photo processing in AUTOCAD 2011 to measure deflection..... 52
Figure 2-32 Change in the horizontal diameter of the pipeline with respect to the original pipe diameter in each installation phase..... 53
Figure 2-33 Change in the vertical diameter of the pipeline with respect to the original pipe diameter in each installation phase..... 53
Figure 2-34 Typical view of the profiler software 54
Figure 2-35 Profiler software analyzing a deformed ring and an un-deformed ring taken from a single frame from a sample video recording..... 55

Figure 2-36 Percent change in the vertical and horizontal diameter across the prove-out section by Laser Video Profile method 56
Figure 2-37 Percent change in the maximum deflection across the prove-out section by Laser Video Profile method 56
Figure 2-38 Percent change in the minimum deflection across the prove-out section by Laser Video Profile method 57
Figure 2-39 Travelling batch plant 58
Figure 2-40 Sample CLSM produced by the automated travelling batch plant 58
Figure 2-41 Casting procedure of CLSM beam and cylinder molds (a) pouring CLSM in mold (b) Filling mold with CLSM (c) Leveling surface for smoothness (d) Molds set for curing 59
Figure 2-42 CLSM specimen beam flexure test by MTS machine (a) test set-up (b) after failure 60
Figure 2-43 Capping of specimen (a) Sulfur capping (b) Specimen damaged during sulfur capping 61
Figure 2-44 Specimen failure 61
Figure 2-45 Load-deflection graph for the 4 CLSM specimens 63

List of Tables

Table 1-1 Parameter comparisons between rigid and flexible pipe design from Durability and Performance of Gravity Pipes: A State-of-the-Art Literature Review (Zhao et al. 1998) 4

Table 1-2 Comparisons between typical CLSM and compacted backfill soil properties .. 18

Table 1-3 Test procedure to determine In-place density and strength of CLSM mixtures, from ACI 229R-99 20

Table 2-1 Schedule for deflection measurements based on the MOP-119 and laser photo method 29

Table 2-2 Summary of the pipe and pipeline physical properties 30

Table 2-3 Pipe lengths and sections per pipe 30

Table 2-4 Percent average change in pipe diameter per installation phase 51

Table 2-5 Compressive strength test results 62

Chapter 1

Introduction, Literature review, Objective

1.1 Introduction

The history of buried pipes dates back to thousands of years ago. Iron pipes were first developed in England in 1824. Steel pipes were born after the introduction of the Bessemer process. In 1861 the development of the open-hearth furnace enabled steel to be produced in tons. The design of buried pipes began in the year 1913 when Anson Marston derived an equation for soil load on pipe. The concept of pipe-soil interaction was brought about by Spangler in 1941, who further derived the Iowa Formula that predicts the horizontal displacement of buried flexible pipe based on E' (horizontal soil modulus). The E' value was later improved by Watkins who rederived the formula to the Modified Iowa Formula to show that ring deflection is principally controlled by soil and not by the pipe. The practical theory that crack width should not exceed 0.01 inch "hundredth inch crack" was brought about by William. The first steel pipes with cement mortar lining were produced in the 1960's which helped against corrosion and increased ring stiffness. With the introduction of the American Water Works Association (AWWA) and American Society for Testing Materials (ASTM) standards and manuals have been produced to aid steel pipe design, such as ASCE Steel Pipe Manual of Practice (MOP-119) and AWWA Manual 11 (M11).

1.1.1 Pipe Mechanics and Installation

Figure 1-1 shows a schematic of the typical terminologies used in pipe and trench configurations from ASCE Buried Flexible Steel Pipe (2009).

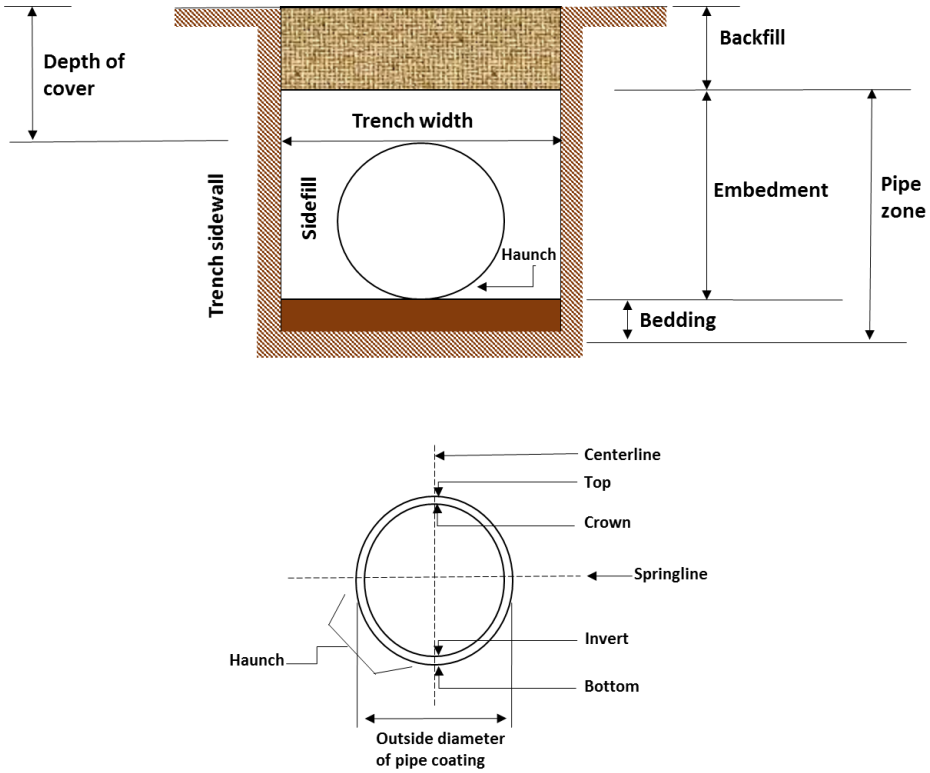

Figure 1-1 Schematic of the typical terminologies used in pipe and trench configurations from ASCE Buried Flexible Steel Pipe (2009)

The structural performance of buried pipes depends on the pipe material and the properties of the soil surrounding it. Pipes have to withstand the internal pressure of the fluid and the external loads applied by the soil backfill around the pipe. Pipe materials hence play an important role in the structural design of pipes. Other considerations to take into account when selecting pipe material include; condition of native soil, availability, corrosion resistance, maintenance and bedding requirement, as described by Jeyapalan (2007). Pressure pipes are generally considered to be in one of two main categories: rigid or flexible. In rigid pipe design, the internal and external forces are analyzed together to evaluate the stresses created by bending and thrust forces on the pipe wall. The pipe wall is then designed to resist these forces. Examples of rigid pipe

include reinforced concrete, vitrified clay and Prestressed Concrete Cylinder Pipe (PCCP). In flexible pipe design, the pipe depends on the surrounding soil envelop to form a composite soil-structure system that can carry the loads that cause excessive deflection and buckling. Examples of flexible pipe include steel, ductile iron, corrugated steel and polyethylene. Table 1-1 shows the comparison of some of the key parameters between rigid and flexible pipe design from Durability and Performance of Gravity Pipes: A State-of-the-Art Literature Review (Zhao et al. 1998). Steel pipe design is governed by two standards namely AWWA C200 and M11. AWWA has limited pipe deflection to 2 to 5 percent of the pipe diameter for various lining types; for cement mortar lining it is 2 percent. The accepted design stress for water steel pipes is 50% of the minimum yield stress (AWWA M11, 2004).

The Occupational Safety and Health Act (OSHA) requires that all trenches that exceed 5 feet (1.52 meters) depth be shored. Figure 1-2 shows trench shield used in a segment of the prove-out section to protect the trench from excavation. Pipe installation is normally assembled in the trench, and pipes should be laid to lines and grades as per specifications. Sandbags can be used beneath the pipeline to assist in placement and even flow of CLSM around the pipe bedding, as shown in Figure 1-3.

Table 1-1 Parameter comparisons between rigid and flexible pipe design from Durability and Performance of Gravity Pipes: A State-of-the-Art Literature Review (Zhao et al. 1998)

Parameters	Rigid pipe	Flexible pipe
Earth Load	Marston load	Prism load
Load Carrying Mechanism	Support earth load by inherent strength in the pipe material.	Rely on lateral soil resistance for stability and support to carry earth load.
Bedding and Backfill	Important in distributing the load and minimizing stress concentrations.	Critical, and part of pipe load-carrying system.
Design Approach	Strength governs. Three-edge-bearing strength is used. Earth load is determined by Marston's equation.	Deflection governs. Strain is a critical factor. Deflection can be determined by Spangler's equation.
Creep	Negligible	All plastic pipes have decreasing modulus of elasticity, with time, when subjected to sustained loads.

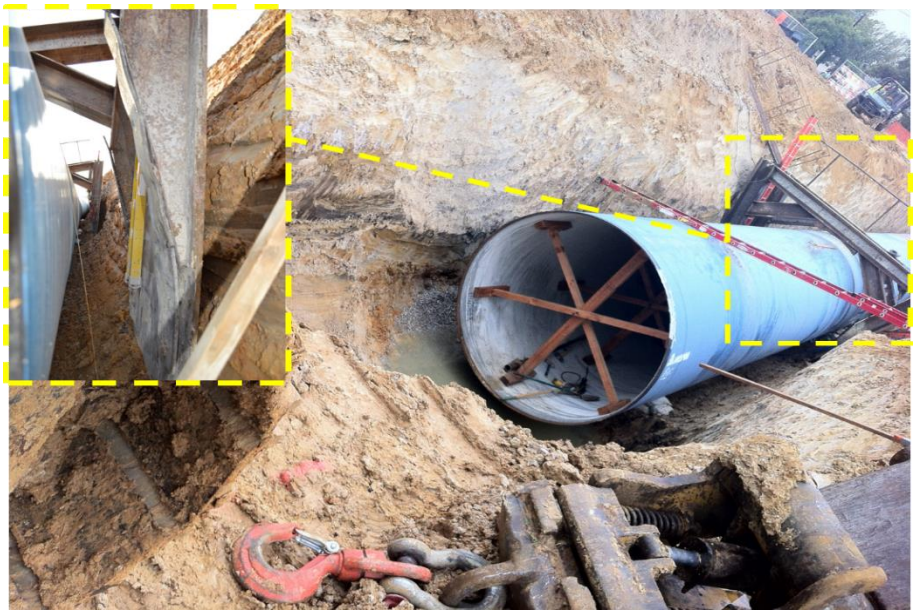

Figure 1-2 Steel trench shield to protect the trench walls from collapsing while excavating

Figure 1-3 Sandbag placement beneath pipe

Backfilling and compaction of selected soil materials are important factors in maintaining structural integrity of the pipe; moreover, analyzing pipe behavior is one of

the priorities during installation of pipelines. Using native materials as backfill material is beneficial to the cost and design of the project. Figure 1-4 below shows native backfill on the pipeline in the prove-out section after CLSM was used as an embedment. Trenches need to be wide enough for proper soil placement. The trench width of the prove-out section varied from 13.00-17.33 ft. (3.96-5.28 m) measured at the spring line. The reason for the variation was to accommodate enough space at the pipe joints for installation work. Figure 1-5 shows the trench width along the pipeline.

Figure 1-4 Backfilling of prove-out section using native soil

Figure 1-5 Trench configuration used in the section J of IPL

According to Jeyapalan (2007), our least most expansive construction material steel and ductile iron are the ones most susceptible to degradation from the natural environment. Different types of protective coating (Epoxy, Tapes, Cement Mortar and Metallic) are used to isolate the susceptible steel from the environment. Since the 1940's cement mortar has been used as protective coating and lining for steel pipes. Cement mortar is typically composed of Portland cement, sand and water, reinforced with wire (Steel pipe: a guide for design and installation, 2004). Cement mortar forms an iron oxide layer that inhibits corrosion when held in contact with the surface of steel pipe. The continuous contact of steel and cement mortar is therefore important for pipe design as it increase pipe wall stiffness. It is essential to limit deflection in these pipes to prevent excessive cracking to the cement mortar. The standard for cement mortar protective lining and coating for steel water pipe 4 inch and larger (AWWA C205) provides a complete guide for the use of mortar lining and coating. Cement mortar has been used as a protective median on the steel pipes of the prove-out section. The steel pipe thickness

is 0.47 inch (11.9 mm) and the cement mortar thickness about 0.5 inch + 1/16 inch (12.7 mm +1.58 mm). Figure 1-6 shows the cross section view of the steel pipe and cement mortar in the prove-out section.

Figure 1-6 Cross section view of bond between steel pipes and cement mortar

To prevent excessive deflection and out-of-roundness during pipe installation, especially after lining and coating have been applied, temporary supports may be utilized like wooden stulls and steel bracing. Internal bracing with steel and wooden stulls may be necessary in backfill conditions and should not be removed until the compacted backfill is placed to provide ample lateral support to the pipe. Stulls should be placed 15-20% of total pipe length per section and at least 4 feet (1.2 m) away from pipe end (ASCE MOP-79). Figure 1-7 shows the various wooden stull configurations in the prove-out section used during the CLSM installation phase, and Figure 1-8 shows the configuration of steel bracing used to minimize deflection during backfilling.

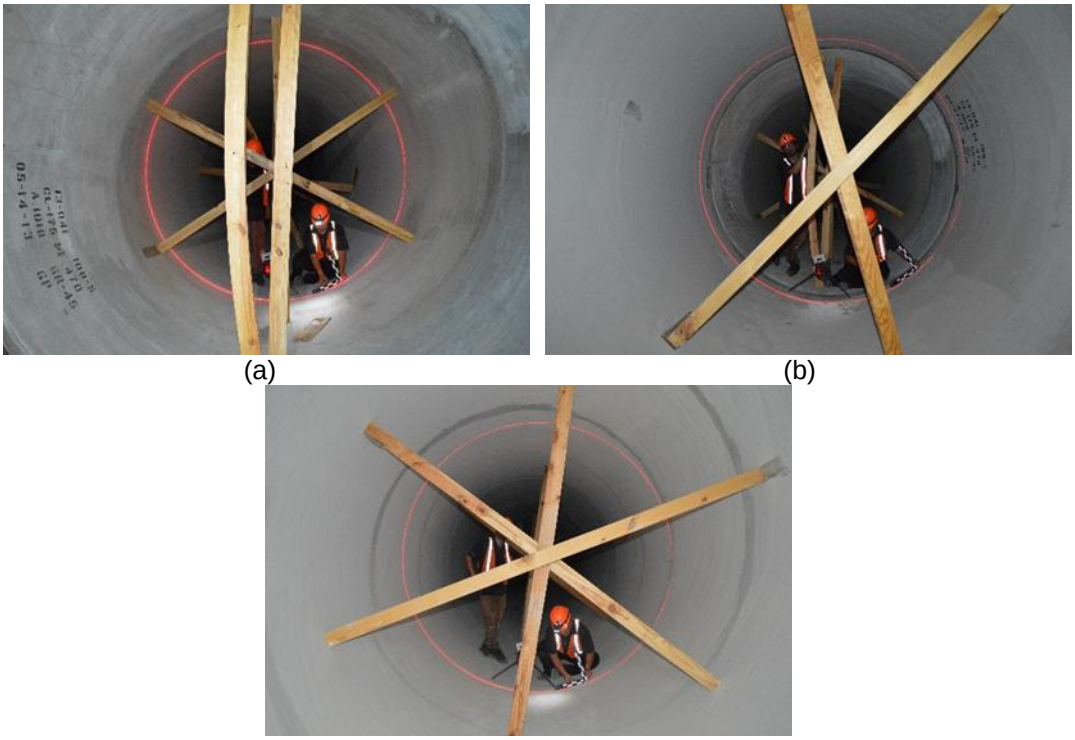

(a) (b)

(c)

Figure 1-7 Wooden stull configurations (a) Vertical (b) Crossed (c) Three legs

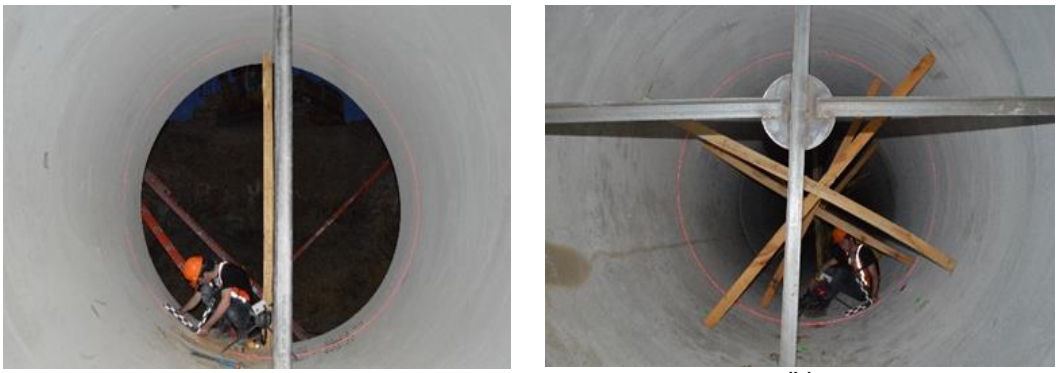

(a) (b)

Figure 1-8 Configuration of steel bracing (a) Vertical (b) Crossed

The need for care in the placement of pipe, compacted bedding and embedment is obvious. Cracks in the cement mortar may reduce the pipe ring stiffness, which is a major concern during handling and installation. After installation, the surrounding soil

holds the pipe in shape and ring deflection is nearly equal to vertical strain of the side-fill soil (Buried Flexible Steel Pipe, 2009).

1.1.2 Pipe Design

While the behavior of large diameter steel pipes during installation is the emphasis of this study, knowing the design concept of pipes is key to understanding pipe structural integrity. In flexible pipe design, external and internal loads are analyzed separately. The first step in buried steel pipe design is to use hydraulic equations (Hazen-Williams, Manning and Scobey formula) to calculate flow in pipes and design pipe size. The next step is to determine wall thickness required for internal pressure; then to check if the wall thickness is sufficiently stiff for handling. Lastly, it is essential to determine the maximum external loads depending on pipe embedment. Structural design of welded steel pipes is based on principles of pipe performance and the conditions for performance limit as described by the ASCE Buried Flexible Steel Pipe (2009). The M11 standard which is published by AWWA has been used for design and performance of steel pipes.

To compute steel pipe wall thickness, a set value for internal pressure is analyzed by limiting the hoop tensile stress in the steel. For design considerations, the most common internal pressure analyzed is operating pressure (Pw), which limits the allowable hoop tensile stress to 50% of the minimum yield strength of the material. Ring stiffness is resistance to deflection; pipe stiffness is defined as the ratio of concentrated load applied to a cylinder over the resulting deflection, as described by Buried Flexible Steel Pipe (2009). Ring compression stress is present in pipe wall if the pipe ring is held in a circular shape when external pressure is applied. Performance limit for common pipe diameters and thicknesses is wall crashing or buckling at yield stress, σY, Buried Flexible Steel Pipe (2009). Ring deflection is neglected, as the value is usually limited by specification. Yield stress is considered a conservative performance limit for design as

steel is ductile. Biaxial yield stress should be taken into account for steel pipes and is caused by longitudinal stresses, σz.

The AWWA Steel Pipe: A Guide for Design and Installation, M11 (2004) and Buried Flexible Steel Pipe (2009) describe the design of wall thickness (t) for steel cylinder, depending on the internal design pressure, and limiting steel stresses due to internal pressure.

$$t = \frac{pd}{2s} \tag{1.1}$$

Where,

t = minimum pipe wall thickness for the specified internal pressure, in

p = internal design pressure, working pressure (Pw) or surge pressure (Ps), psi

d = outside diameter, in

s = stress internal pressure, psi, for PWORKING ($s = 0.5\sigma y$) for PSURGE ($s = 0.75\sigma y$)

The design of the minimum wall thickness for handling is based on three following equations:

For pipe sizes I.D. up to 54in: $t = \frac{D}{288}$ (1.2)

For pipe sizes I.D. greater than 54in: $t = \frac{D+20}{400}$ (1.3)

For mortar-lined and flexible coated steel pipe: $t = \frac{D}{240}$ (1.4)

The Modified Iowa deflection formula, Equation 1.6, predicts the pipe deflection. The modulus of soil reaction (E') used in this formula is an empirical value that indicates the stiffness of the soil embedment. Values for E' for different soil types and compaction levels can be found in AWWA M11 and tests conducted from Howard (2006).

$$\text{Deflection} = \frac{\text{LOAD}}{\text{PIPE STIFFNESS+SOIL STIFFNESS}} \tag{1.5}$$

$$\Delta x = Dl \frac{KWr^3}{EI+0.061E'r^3} \quad (1.6)$$

Where,

Δx = horizontal deflection of pipe, in

Dl = deflection lag factor (1.0-1.5)

K = bedding constant (0.1)

W = load per unit of pipe length (lb/ linear in)

r = radius, in

EI = pipe wall stiffness

E = modulus of elasticity , for steel 30,000,000 psi (20,6841 MPa)

I = transverse moment of inertia per unit length of individual pipe wall components $t^3/12$, t = pipe wall thickness, in

E' = modulus of soil reaction, psi

The M11 has limited pipe deflection to allowable limits for the various lining and coating systems. The allowable deflection for pipes with mortar-lined and coating is two percent (2%) of pipe diameter, mortar-lined with flexible coating is three percent (3%) and five percent (5%) for flexible coating and lining. Small cracks less than 1/16 inch (1.58 mm) are usually present in mortar lining and coating but are not critical, as they close by autogenously healing in a moist environment. Once pressurized, pipes tend to reround and close cracks due to deflection caused by installation. The tensile zone of the pipe is where the widest cracks occur, at the springline for coatings and at the crown and invert for linings, Buried Flexible Steel Pipe (2009). Figure 1-9 shows various small cracks in the prove-out section formed during mortar placement, pipe handling and during the installation phase.

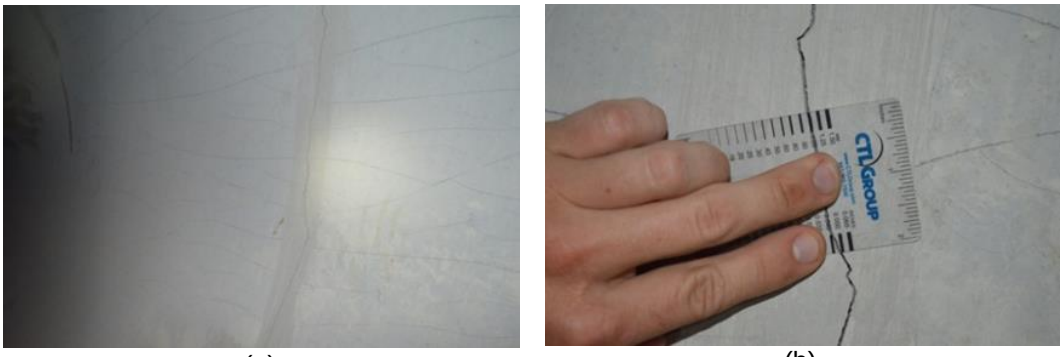

(a) (b)

(c)

Figure 1-9 Types of cracks observed in prove out-section (a) Small longitudinal cracks (b) 1 inch crack (c) Circumferential crack

ASCE MOP-119 (2009) has introduced the following equations below for predicting the widest possible single crack width, w.

$$\frac{\mathrm{w}}{2t_c} = \frac{1}{r_{min}} - \frac{1}{\mathrm{r}} \tag{1.7}$$

$$\frac{\mathrm{w}}{2t_l} = \frac{1}{\mathrm{r}} - \frac{1}{r_{max}} \tag{1.8}$$

Where,

w = width of crack, in

t_c = thickness of mortar coating, in

r_{min} = minimum radius, in

t_l = thickness of mortar lining, in

r = circular radius of pipe, in

r_{max} = maximum radius, in

The radius of curvature must be measured, especially in deformed pipe. MOP-119 introduced a simple method to calculate pipe deflection during installation. This method can be done from either inside or outside of the pipe. From outside the pipe, a rod with a fixed length (L) is placed on top of the pipe crown, and then the perpendicular distance between the ends of each side of the rod and the pipe wall, e' and e'', will be obtained. From inside the pipe, the rod should touch the pipe's interior wall at two points to obtain the perpendicular distance e (Middle Coordinate) between the center of the rod and the pipe wall. The radius of curvature of the deflected pipe at different locations is calculated by using Equation 1.9, and the graph from Figure 1-10 will be used to estimate the maximum deflection in the pipe.

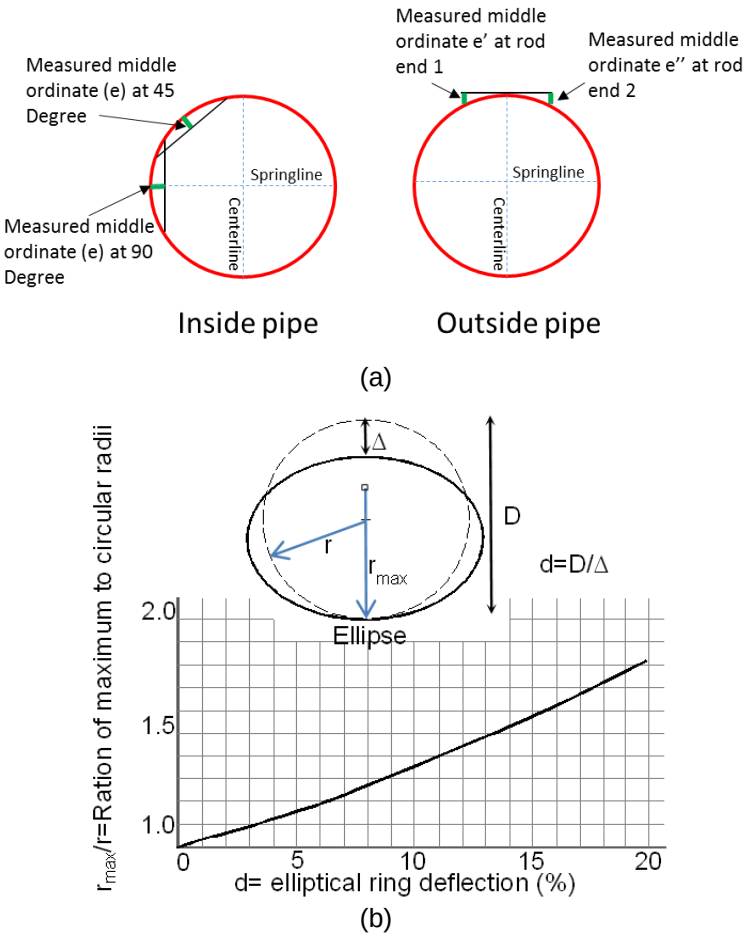

Figure 1-10 Maximum deflection estimation (a) Schematic location of middle ordinate (b) Relationship of ratio of radii to elliptical ring deflection courtesy of MOP-119

$$r = \frac{(4e^2+L^2)}{8e} \tag{1.9}$$

Where,

r = radius of curvature, in

e = middle coordinate, in

L = cord length, in

Typically, the maximum deformation of a given pipeline section occurs in the X or Y diameter (symmetric); however, the pipeline may deform in a skew manner so as to

have the maximum deformation in the diagonal direction of the pipe, as shown in Figure 1-11. The maximum deformation is captured by ovality graphs for this racking behavior. Ovality shows how elliptical the cross-section of a pipe has become due to deformation. This is displayed as a positive percentage, where 0% represents a perfectly round pipe. In this study the maximum of X and Y deformations and the ovality of the pipe are considered for the maximum deformation of the pipeline. A formula for pipe ovality is given by the American Society for Testing and Materials standards (ASTM F1216-09) and is shown in Equation 1.10 below. For the mean inside diameter, software (i.e. profiler software) can be used to get values at varying points per section.

$$q(ovality) = 100 \times \frac{Maximum\ inside\ diameter - Mean\ inside\ diamter}{Mean\ inside\ diamter} \quad (1.10)$$

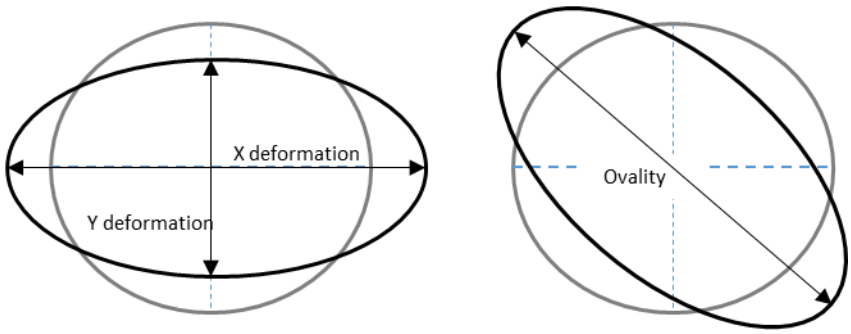

Figure 1-11 Schematic of symmetric and unsymmetrical deformations observed in pipeline

1.1.3 Controlled Low Strength Material

The importance of selecting the correct type of backfill material in flexible pipe design should not be underestimated as the pipe stiffness is negligible compared to the backfill material. There are several backfilling options available (treated native soil, compacted native soil and select fill) depending on specific site conditions. One of these materials is Controlled Low Strength Material (CLSM). CLSM is a self-compacted,

cementitious material used primarily as a backfill in place of compacted fill (ACI 229-R-99). CLSM is defined by ACI 116R-00 as materials that result in a compressive strength of 1200 psi (8.3 MPa) or less. Most applications of CLSM require unconfined compressive strengths to be between 40 psi to 300 psi, to allow for future excavations and carry the sustained loads. CLSM may also be referred to as flowable fill and does not only depend on the surrounding soil properties but also on the pipe properties. ASTM D 4832 states that CLSM transfers the load from the pipe to the in situ material, so the native soil must be able to provide the necessary support for the pipe. CLSM may be used as an embedment material or as a backfill material. It works as gap filler or a trench filler when used as an embedment material. If compacted soil is not used, CLSM is the main form of support for flexible pipe. Table 1-2 shows key property comparisons between typical CLSM and compacted backfill soil. ASCE Buried Flexible Steel Pipe Design and Structural Analysis (2009) shows an increase in compressive strength of plain granular soil when the same granular soil is mixed with cement, an increase of σx from 30 psi to 100 psi, as shown in Figure 1-12.

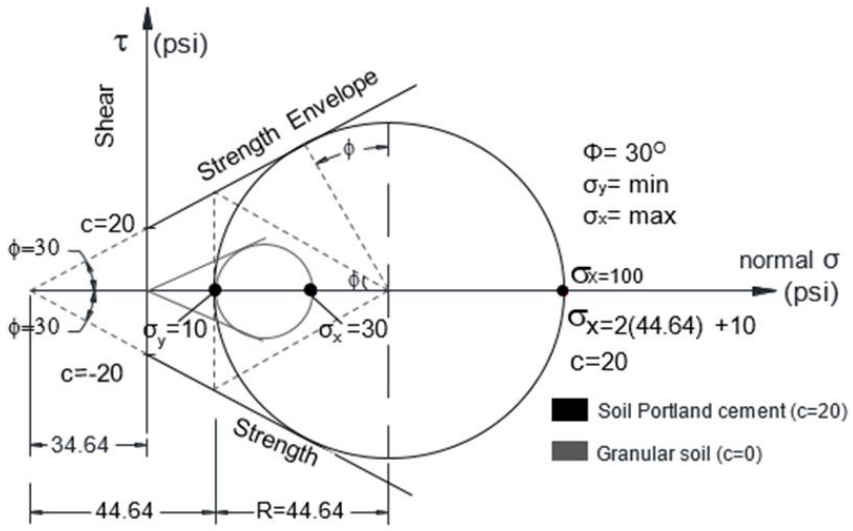

Figure 1-12 Comparison of maximum principal stresses between Granular soil with and without Portland cement from ASCE Buried Flexible Pipe (2009)

Table 1-2 Comparisons between typical CLSM and compacted backfill soil properties

Properties	CLSM	Compacted backfill soil
Placement	Self-leveling	Compaction needed
Density	115-145 pcf (1842-2322 kg/m3)	100-125 pcf (1601-2002 kg/m3)
28-Day compressive strength	< 1200 psi , 300 psi (<8.27 MPa, 2.06 MPa)	50-100 psi (0.34-0.68 MPa)

Advantages of CLSM as described by (Smith,1991), are that is is readily available using locally available materials; easy to deliver using truck mixers; easy to place, as CLSM is self-leveling; strong and durable, as load carry capacity of CLSM is typically higher than compacted soil; more resistant to erosion; will not settle under loading; reduces excavation costs, as narrow trenches can be made; improves worker

safety, as workers do not need to enter the trench; can be excavated and requires less field testing than soil backfill. Design concerns with the use of CLSM include pipe flotation, which depends on the height which the flow reaches and weight of pipe. This can be mitigated by pouring the CLSM in lifts that control the volume of CLSM entering the trench and create an adhesion between the pipe and existing level of CLSM. During construction, care should be taken that CLSM is placed evenly on both sides of the pipe to prevent pipe movement and extra stress exerted on the pipe. Testing the strength of CLSM is usually carried out 7 days from when the mix was used and this delay in time makes it difficult to correct any potential problems revealed in testing, as the pipe is overfilled by this time. Standard testing procedures for CLSM mixtures are shown in Table 1-3, courtesy of ACI 229R-99.

Table 1-3 Test procedure to determine In-place density and strength of CLSM mixtures, from ACI 229R-99

ASTM D 6024	"Standard Test Method for Ball Drop on Controlled Low Strength Material to Determine Suitability for Load Application." This specification covers determination of ability of CLSM to withstand loading by repeatedly dropping metal weight onto in-place material.
ASTM C 403	"Time of Setting of Concrete Mixtures by Penetration Resistance." This test measures degree of hardness of CLSM. California Department of Transportation requires penetration number of 650 before allowing pavement surface to be placed.
ASTM D 4832	"Preparation and Testing of Soil-Cement Slurry Test Cylinders." This test is used for molding cylinders and determining compressive strength of hardened CLSM.
ASTM D 1196	"Nonrepetitive Static Plate Load Tests of Soils and Flexible Pavement Components for Use in Evaluation and Design of Airport and Highway Pavements." This test is used to determine modulus of subgrade reaction (K values).
ASTM D 4429	"Bearing Ratio of Soils in Place." This test is used to determine relative strength of CLSM in place.

1.2 Literature Review

The MOP-119 method is based on ASCE Manuals and Reports on Engineering Practice No.119. The laser profiling method has been used before and several studies have been carried out on this inspection method.

A detailed study was carried out by Abolmaali et al. (2010) to investigate the structural integrity of various HDPE pipelines across ten (10) different states in America. One hundred and ninety-one (191) HDPE pipelines (more than 31,000 feet) were inspected using a high intensity camera and laser profiling unit. It was observed that at least one of the following failure modes (cracking, buckling, inverse curvature, joint displacement and excessive deformation) was present in each pipeline. It was also noted that corrugation growth was present in all pipelines. The data was processed and analyzed to check for deformation. It was reported that 68% of the pipelines inspected deformed more than the allowed limit of 5% (AWWA), with an average maximum deformation of 7.6%. The study showed that the structural integrity of the HDPE pipes monitored were below acceptable levels of service and that video inspection with laser profile is a good practice to verify quality control and quality assurance of pipeline installation.

An independent study conducted by the Kentucky Transportation Center and Pipeline and Drainage Consultant (2006) evaluated the long term performance of HDPE pipes on existing Kentucky DOT HDPE pipelines. Seven (7) sites across Kentucky, measuring 3,892 feet of HDPE pipeline, were selected to be inspected with video inspection, using high intensity lighting (CUES OZ II camera) and profiler laser ring. The data was then processed and analyzed for pipe ovality and possible structural defects. It was reported that corrugation growth increased after installation, with an average maximum corrugation of 0.5 inches, which as a result doubled the manufactures design value for Manning's roughness coefficient (n). Radial cracking was observed in nearly 20% of the pipe sections, while sagging and ponding were observed at 26%. Racking was also observed in the pipelines and the majority of the pipes inspected did not fall within the 5% AWWA deflection limit. This study shows the importance of proper HDPE

pipe installations with respect to long term performance and the need for more frequent inspection of existing pipelines. The advantages of pipe inspection with video and laser profile as compared to mandrel testing was also noted.

Another study was conducted by Pipeline and Drainage Consultants (2006) on preexisting HDPE pipelines in various locations in the state of Ohio. Eleven (11) sites comprised of 672 feet of HDPE pipeline were inspected by manual (physical inspection of vertical and horizontal deflections) and video evaluation (video inspection with CUES OZ II with profiler laser ring). The results were compared to the evaluation of the same pipelines carried out in the year 2001. The advantage of video-laser inspection with respect to mandrel testing was noted as video inspection was able to show significant information in relation to observed defects (cracking, buckling, tearing and sagging). HDPE pipe corrugation growth was reported to be present in the pipelines. Various types of cracking (radial, longitudinal and diagonal) were observed, accounting for at least four times the amount reported in 2001. It was noted that most of the pipes have continued to creep from the previous inspection in 2001 and as result had deflection values higher than the allowed 5% AWWA limit.

A study was carried out by Duran and Seneviratne (2003) to introduce laser-based transducer with automated analysis techniques to evaluate pipe inspection as compared to the use of conventional closed-circuit television cameras (CCTV). The drawback of the use of CCTV was noted essentially by poor image quality produced due to varying lighting conditions and the time consuming process of assessing the images; which are also prone to human error. The use of laser ring profilers is mentioned and analysis with algorithm (ellipse-fitting) is carried out to detect steep changes in the image intensity. These changes are then monitored as potential defect regions in the pipe line. A variety of pipes were inspected, and it was concluded that the laser profile system,

when used in conjunction with CCTV, is a more complete and effective system than the latter method alone.

The research of Bosseler and Stein (1998) states that in flexible pipe design, there is emphasis on vertical and horizontal deflection, while neglecting the overall instant or over-time variations (i.e. rotated ellipse) in the geometric pipe shape. A parameter system was established to describe the rate of deflection and to verify its accuracy. False measurements were identified by using a model of a linear elastic ring. It was also noted that empirical approaches alone do not give a complete solution to probable cause of defect. It was concluded that the use of the parameter system is more valuable when empirical methods show that the measured deflections do not meet design requirements.

The Iowa formula is a good approach to measure pipe deflection via numerical analysis, Finite Element Analysis Method (FEM) can be used in conjunction with formula to demonstrate both deflection and pipe-soil interaction. Several papers have been written about the use of FEM in buried pipe analysis, Dezfooli (2013) used three dimensional finite element modeling on large diameter steel pipes via experimental soil box tests carried out by Sharma et al. (2011) at the University of Texas at Arlington. The model was able to successfully predict horizontal and vertical deflections during stage construction. Two stage constructions were tested based on the soil box tests: pea gravel for bedding with native soil for backfill and lime treated native soil for bedding with native soil for backfill.

Another study by Bellaver (2013) aims at showing the structural integrity of large diameter steel pipes embedded with CLSM for the Integrate Pipeline Project (IPL) in Texas and comparing the field results with a nonlinear three dimensional finite element model. Strain gauges monitored displacement and strain for up to 350 days for 3 buried pipes with varying trench widths and level of embedment of CLSM at 30% and 70% pipe

diameter. The data obtained was used to verify the FEM model developed. It was concluded that he FEM model was able to successfully replicate the field test.

CLSM has been the interest of many research studies. A study was carried out by Boschert and Butler (2013) to show that conventional equations (Marston, Modified Marston and Prism load) for calculating backfill loads on pipes are not reliable when CLSM is used as a backfill. Three (3) projects were conducted using Vitrified Clay Pipes (VCP): two (2) pipes with 39 and 24 in. (991 and 610mm) diameters on the field, using strain gauges to record load, and the third, an 8 inch (203mm) in the laboratory, using conventional equations to compute backfill loads. It was observed that neither the Marston equation nor the Modified Marston equation were close to the applied load. These equations were noted too be conservative when CLSM is used. Prism shear was observed contrary to assumption of having a rigid system of pipe and CLSM. It was also observed that the CLSM side fills provided some support to the soil prism above the pipe. The study also showed that the load factor for CLSM is heavily dependent on proper mix design and production. No pipe flotations were observed in the field tests. It was noted that CLSM acted as a Bingham fluid.

Research carried out by Simmons (2002) shows the use of flowable fill as a backfill material around buried pipes of 6 in. (152.4 mm) and 8 in. (203.2 mm) diameter. Fly ash and bottom ash were used in varying amounts to come up with an optimum mix design. Laboratory pipe testing was carried out to test for pipe-soil interaction. It was observed that all mix designs showed problems with segregation. Pipe testing showed that when trench width ratio is increased; deflections and centerline soil stresses decrease. Other observations noted were that high strength CLSM and cohesive soil resulted in less deflection than low strength CLSM and cohesive soil. Numerical analysis was carried out by using Spangler's Iowa equation, and it was concluded that deflections

can be accurately predicted for small diameter pipes with the use of realistic soil stiffness values.

The research of Sharma et al. (2013) presented the response of large diameter thin-walled steel pipe with various embedment conditions. Five tests were carried out on 72inch diameter steel pipes with a diameter-to-thickness ratio (D/t) of 230. The varying embedment soil (natural or lime treated) was from the IPL project in Texas. Strain gauges were used to measure pipe deflection and wall strain. It was observed that none of tests showed both vertical and horizontal deflections as equal, contrary to Spangler's soil pipe interaction model; nor was the assumption that passive soil resistance by the embedment is equal about the springline. It was also noted that the use of modulus of soil (E') is subjective to large diameter pipes and an unfair representation (not based on strength parameter of soil) of fitted E' values. It is also noted that the peaking behavior of pipes during embedment installation is not represented in Spangler's model. It was observed that, in all tests, the deflections due to surcharge load were all below the allowable 3% limit as per AWWA specifications. It was concluded the strength of the native soil treated with lime had improved, hence reducing backfill load and pipe deflection. It was observed that special care should be taken with steel pipes with cement mortar lining to prevent excessive strain formation, especially during the embedment development.

1.3 Objective

The main objective of this research is to compare deflection measurement methods (MOP-119, Laser Photo Profile and Laser Video Profile) for 108 in. (2.74 m) diameter steel pipes embedded with CLSM. To insure structural integrity of the pipeline by limiting pipe deflection to 2 percent of the pipe internal diameter for cement mortar lining as per AWWA specification.

To assess the use of CLSM as a backfill material and test material properties of CLSM. Beam and cylinder CLSM specimens were tested as per Standard Test Method for Flexural Strength of Concrete (Using Simple Beam with Third-Point Loading) (ASTM C78/C78M-10) and Standard Test Method for Preparation and Testing of Controlled Low Strength Material (CLSM) Test Cylinders (ASTM D 4832-10).

1.3.1 Justification of Research

Theory alone cannot be used to predict pipe deflection, due to real field conditions (field personnel experience, equipment used, materials and variations in ground properties); hence, the installation achieved is not always how it is designed to be. For flexible pipes the main performance limit for design is deflection. Deflection needs to be limited for the structural integrity of the pipe. Pipe-soil interaction is necessary in flexible pipe design, and the soil accounts for the majority of the stiffness to resist deflection. The analysis and monitoring of buried steel pipes is thus vital for large diameter flexible pipe

Chapter 2

Field Test

2.1 Introduction

The prove-out section of line J of IPL is located in Kennedale Texas adjacent to Linda road and S Dick Price road. Field tests for pipe deflection measurements were all taken in this location. Figure 2-1 shows an aerial view of the prove-out section. Three (3) methods were used to measure pipe deflection: MOP-119, Laser Photo Profile and Laser Video Profile. MOP-119 method was used in conjunction with Laser Photo Profile method when stulls where present within the pipeline and later with both the Laser Photo and Video Profile methods when stulls were completely removed from the prove-out section. The schedule for deflection measurements was based on the progress of construction of the different phases of pipe installation. Figure 2-2 shows a schematic of the installation phases. Table 2-1 shows the schedule for deflection measurements based on the MOP-119 and Laser Photo Profile method. Laser Video Profile was performed for the entire prove-out section in one visit on September 13th, 2013.

Figure 2-1 Aerial view of the prove-out section and site location

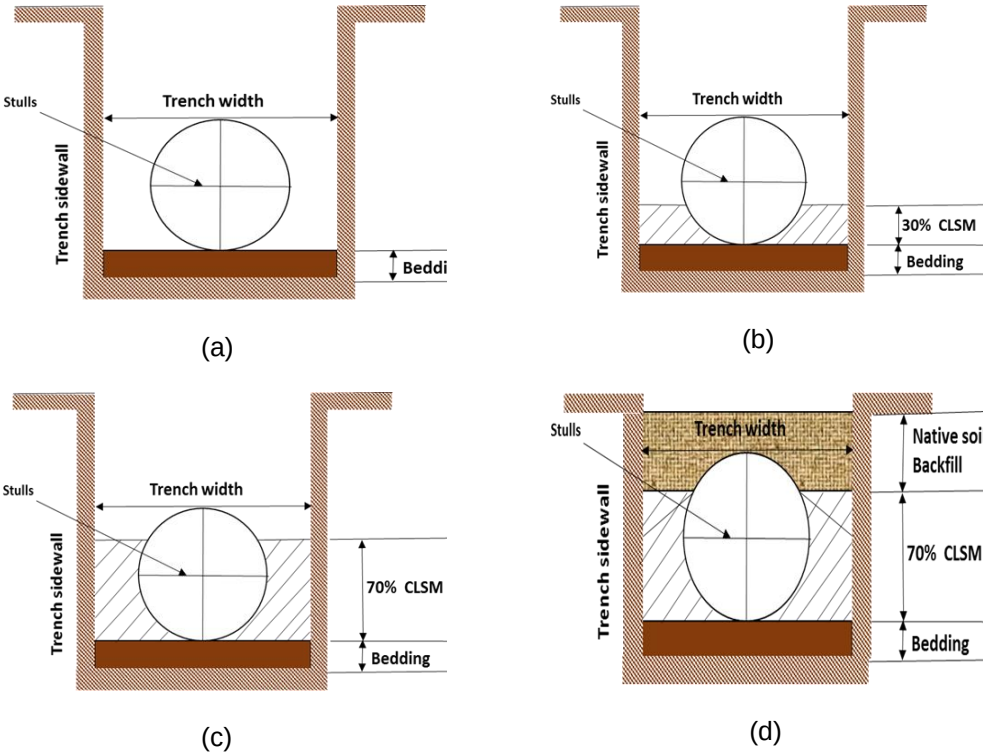

Figure 2-2 Schematic of installation phases (a) placement (b) CLSM embedment at 30% pipe diameter (c) CLSM embedment at 70% pipe diameter (d) backfill

Table 2-1 Schedule for deflection measurements based on the MOP-119 and laser photo method

Installation phases and measurements	0'100'	100'-200'	200'-300'	300'-400'	400'-500'
Pipe Placement	Monday, August 19,2013	Monday, August 19,2013	Monday, August 19,2013	Tuesday, August 20,2013	Tuesday, August 20,2013
30% CLSM	Tuesday, August 20,2013	Wednesday, August 21,2013	Wednesday, August 21,2013	Wednesday, August 21,2013	Thursday, August 22,2013
70% CLSM	Thursday, August 22,2013	Friday, August 23,2013	Friday, August 23,2013	Friday, August 23,2013	Saturday, August 24,2013
Full Backfill	Saturday, August 24,2013	Saturday, August 24,2013	Monday, August 26,2013	Tuesday, August 27,2013	Thursday, August 29,2013

The total number of pipe joints in the prove-out section is eleven (11) with varying joint lengths of 24 to 50 ft. (7.3 to 15.2 m).Table 2-2 shows a summary of the pipe and pipeline physical properties, and Table 2-3 shows the various pipe lengths and sections per pipe where measurements were taken. There were forty-three (43) sections in the prove-out where measurements were taken with the MOP-119 and Laser Photo Profile method. The Laser Video Profile method was run continuously through the entire length

of the prove-out section without any breaks. Figure 2-3 shows a schematic of the three (3) different pipe joint lengths and sections where measurements were taken.

Table 2-2 Summary of the pipe and pipeline physical properties

Number of pipes	11
Total length (ft.)	518
Pipe internal diameter (in.)	108
Pipe thickness (in.)	0.47
Concrete layer (in.)	0.5 + 1/16

Table 2-3 Pipe lengths and sections per pipe

Pipe Number	Length, ft.	Sections per pipe
1066-1072 and1075-1076	50	4
1073	44	4
1074	24	3
Total	518	43

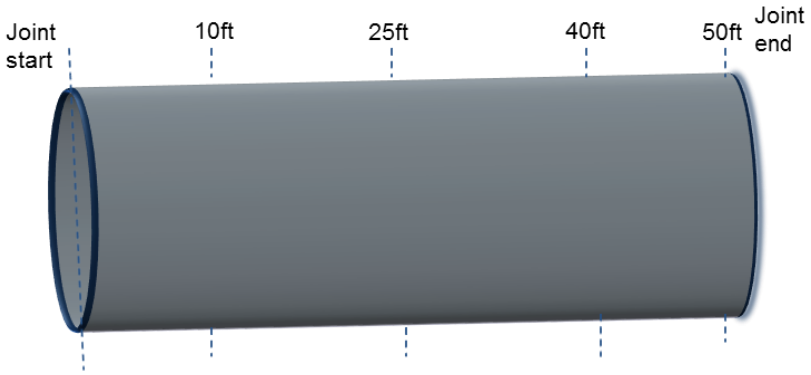

(a)

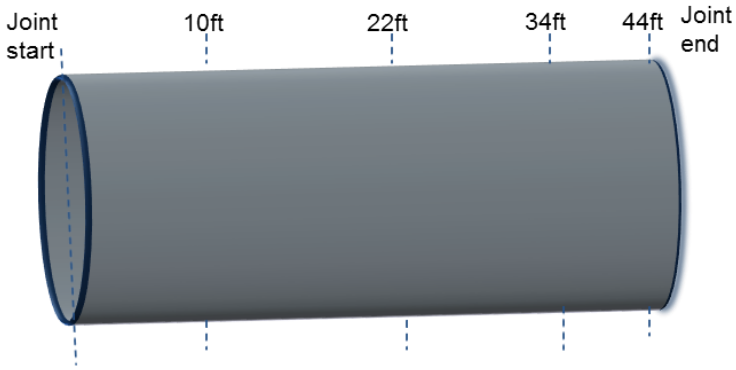

(b)

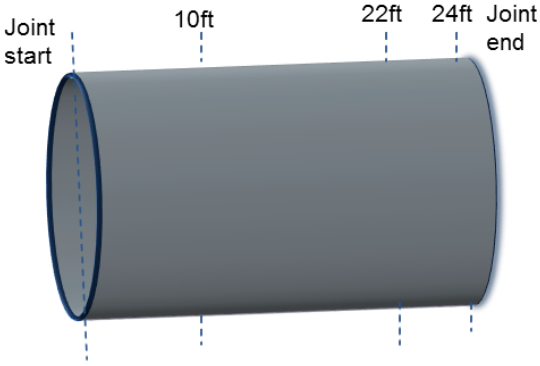

(c)

Figure 2-3 Schematic of the 3 different pipe joint lengths and sections where measurements were taken (a) 50 ft. joint (b) 44 ft. joint (c) 24 ft. joint

The pipes were placed in a narrow trench, less than three times the diameter of the installed pipe (<3d). The use of CLSM as a backfill material allowed for this provision. Figure 2-4 shows placement of the pipes within the trench in the prove-out section.

Figure 2-4 Placement of pipeline within trench

Safety is an important aspect in field tests. All personnel entering the pipeline must obtain a safety training certificate for confined spaced entry. A site supervisor must be present at all times during field measurements. A set of safety equipment and clothing is required for entry to the pipeline as shown in Figure 2-5. An air blower was used to cool the temperature within the pipeline and help with air circulation, Figure 2-6 shows the blower unit used in the prove-out section.

Figure 2-5 Safety equipment and clothing required

Figure 2-6 Blower unit used in the prove-out section

The ports of entry into the pipelines were through manholes. 30 inch (0.76 meter) in diameter. Large measuring equipment needed to be craned into the manhole. Figure

2-7 shows the typical manhole and Figure 2-8 shows personnel and equipment entering pipeline via a manhole.

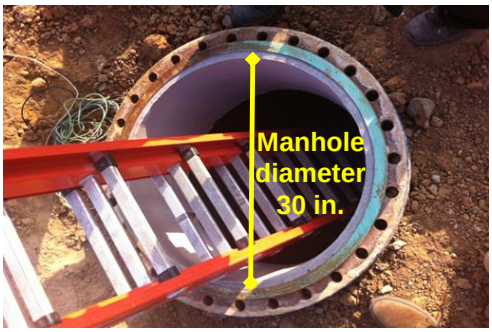

Figure 2-7 30 in. manhole

(a)

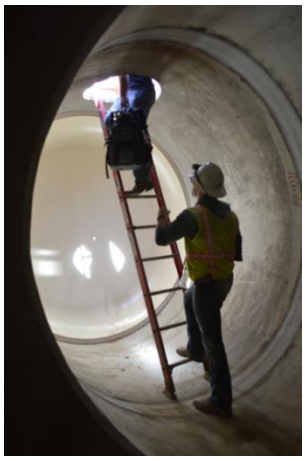

(b)

(c)

Figure 2-8 Personnel and equipment entering manhole (a) equipment craned (b) personnel entering manhole via ladder (c) equipment lowered into manhole

2.2 MOP-119 Method

This method is based on ASCE MOP-119 and is used to measure pipe deflection during installation. A rod with fixed length (L) should touch the pipe's interior wall at two points to obtain the middle ordinate (e), which is the perpendicular distance between the center of the rod and pipe wall. Figure 2-9 shows a schematic of this procedure and where to locate the middle ordinate and pipe radius of curvature.

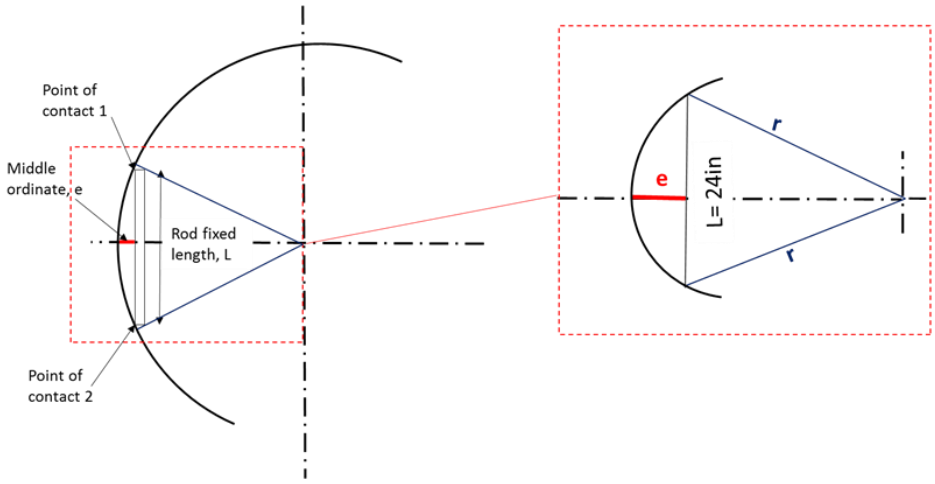

Figure 2-9 Schematic of MOP-119 method for calculating radius of curvature of deformed pipe

The level rod used in this measurement had a fixed length of 24 in. (0.61 m) attached centrically to a digital level rod and digital Vernier caliper. The digital level rod was used to show the angle of rod placement and the digital Vernier caliper to show the measured middle ordinate value, e. Figure 2-10 shows the instrument configuration used to measure the middle ordinate by the MOP-119 method.

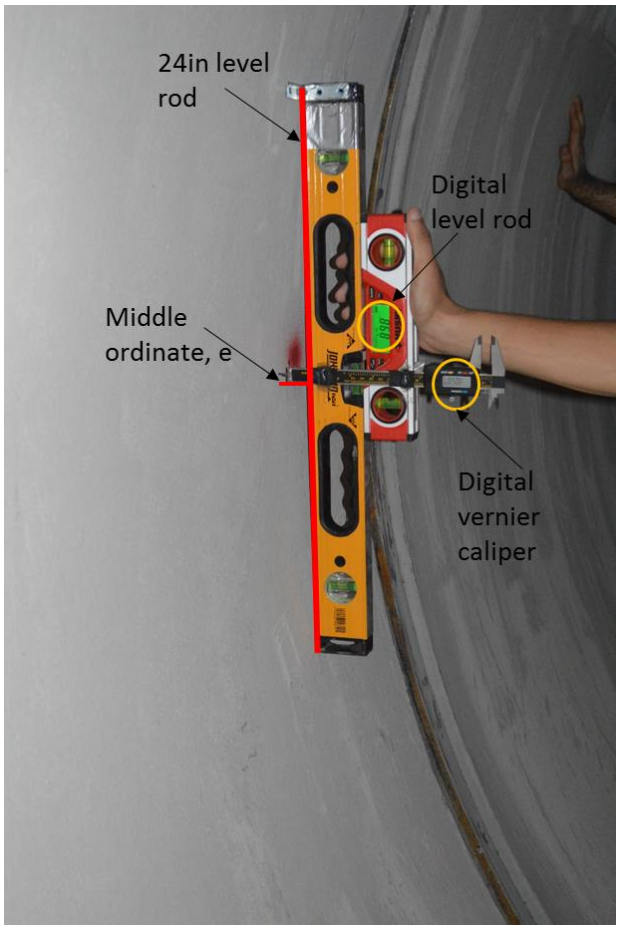

Figure 2-10 Instrument configuration used to measure middle ordinate by MOP-119 method

For each section, two (2) measurements were taken and marked at 90 and 45 degrees from the pipe crown. The 90 degree measurement corresponds to the springline and the 45 degree to where approximately the CLSM layer will end and where maximum stress is expected. Figure 2-11 shows measurements taken per section at 90 and 45 degrees.

(a) (b)

Figure 2-11 Mop-119 measurements taken per section at (a) 90 degree (b) 45 degree

Once the 90 and 45 degree locations were identified with the digital level meter, their positions were marked on the pipe wall with a marker for ease and consistency of repetitive measurements taken at later installation phases. Forty-three (43) sections were measured with this method. The location of each section can be found in Figure 2-3, and the measurements taken at different installation phases can be found in Table 2-1. The middle ordinate (e) values obtained from the digital Vernier caliper were recorded in a sheet for analysis. These values for all the installation phases can be seen in Appendix A for 90 degrees and Appendix B for 45 degrees

2.3 Laser Photo Profile Method

The laser photo profile method was used while stulls were present in the pipeline installation. This method is comprised of a high resolution digital camera, tripod, skid, ten-head laser ring attached to a rechargeable battery and a scale. Figure 2-12 shows the laser photo profile method instrumentation.

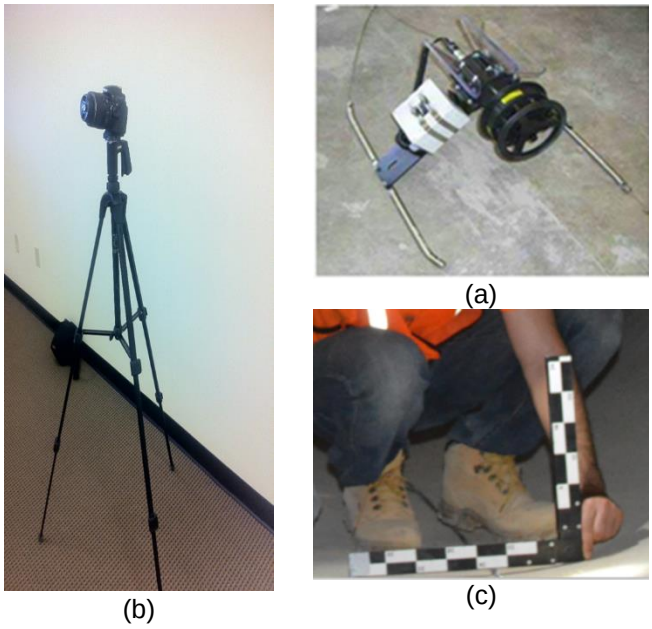

(a)

(b)

(c)

Figure 2-12 Laser photo profile instrumentation (a) ten-head laser ring with rechargable battery on skid (b) high resolution camera on tripod (c) scale

The tripod and camera were set up to stand stable and symmetrical with the pipe's longitudinal axis and at a distance away to capture the entire laser ring profile emitted on the inner surface of pipe wall. The ten-head laser ring was mounted firmly on to the skid, while the rechargeable battery was taped on to the skid for easy access. The skid was checked for stability and placement (symmetrical with pipe axis) before taking shoots. To minimize camera errors based on the location the photos were taken, two fixed points at 90 degrees were marked at equal distance from the joints in order to keep the laser perpendicular to the cross sectioned measured. Figure 2-13 shows placement of skid along the pipe axis symmetry

Figure 2-13 Placement of skid along pipe axis symmetry and stability

Two (2) shoots were taken per section for picture quality assurance and stored in the camera memory card. Forty-three (43) sections were measured with this method, as with the MOP-119 method. The location of each section can be found in Figure 2-3, and the measurements taken at different installation phases can be found in Table 2-1. Figures 2-14 to 2-18 show the laser photo profile method for the 4 sections of the 50 ft pipe joint number 1066 at placement.

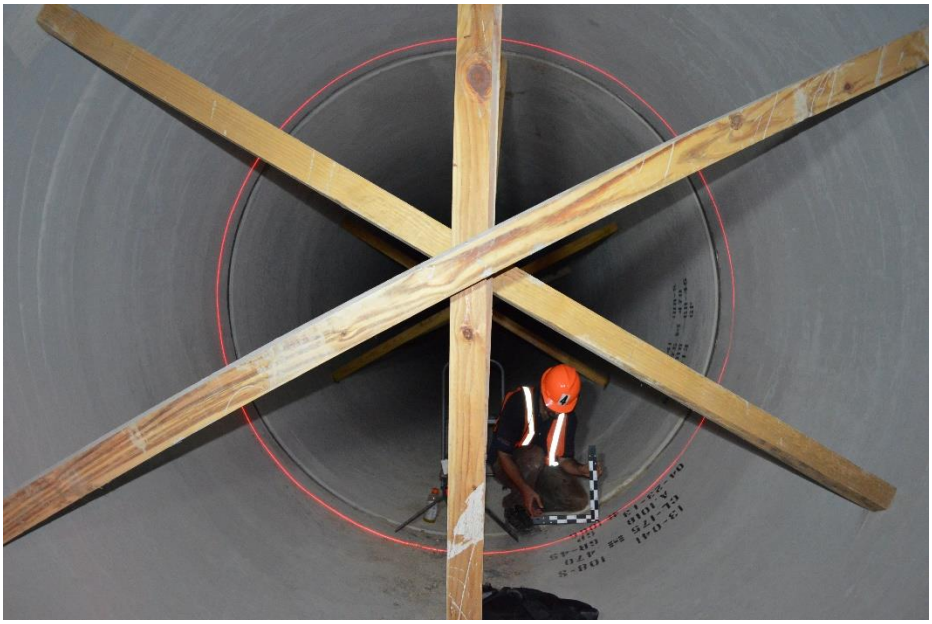

Figure 2-14 Laser photo profile method at start of pipe joint number 1066 at placement

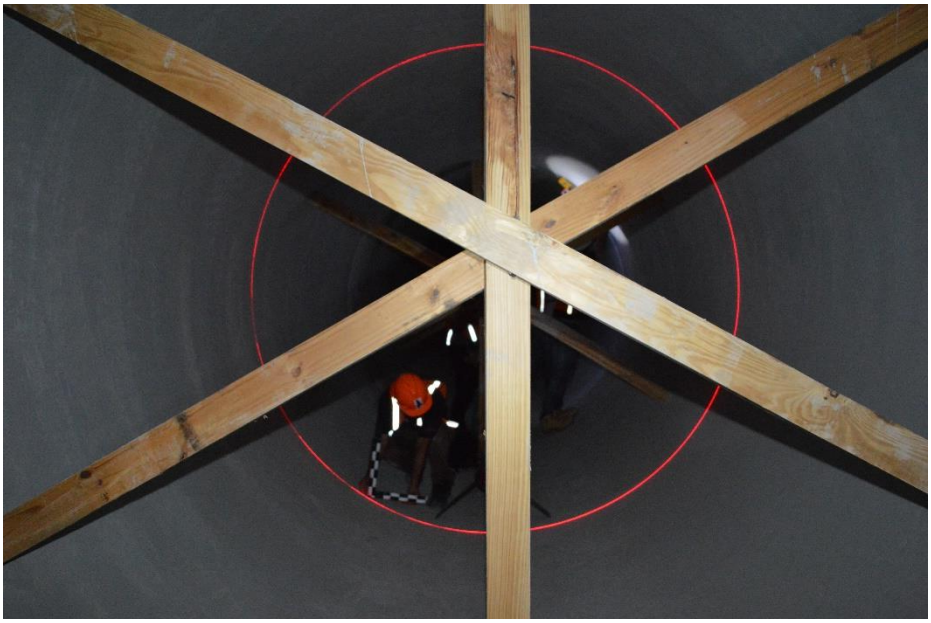

Figure 2-15 Laser photo profile method at 10ft of pipe joint number 1066 at placement

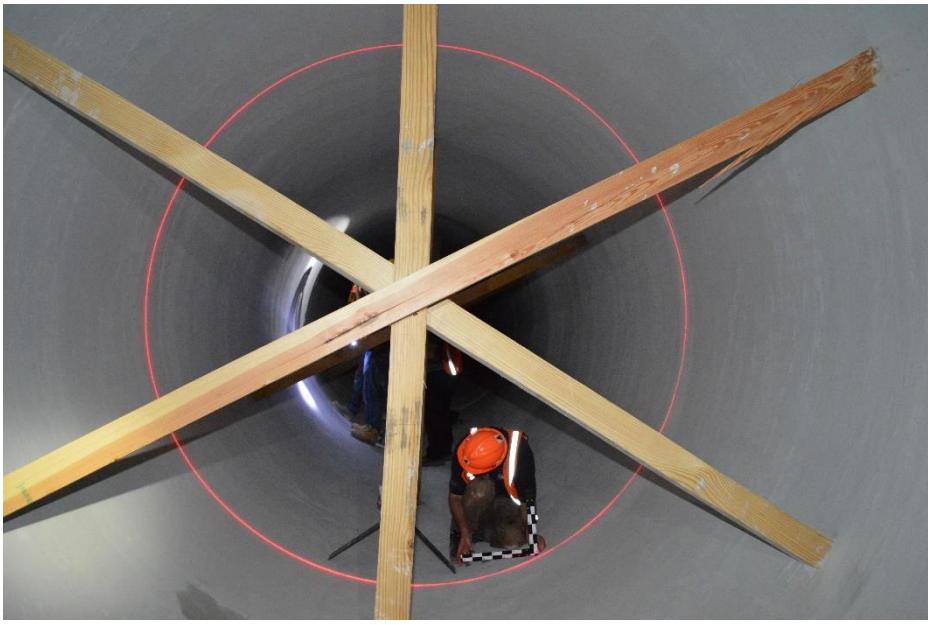

Figure 2-16 Laser photo profile method at 25ft of pipe joint number 1066 at placement

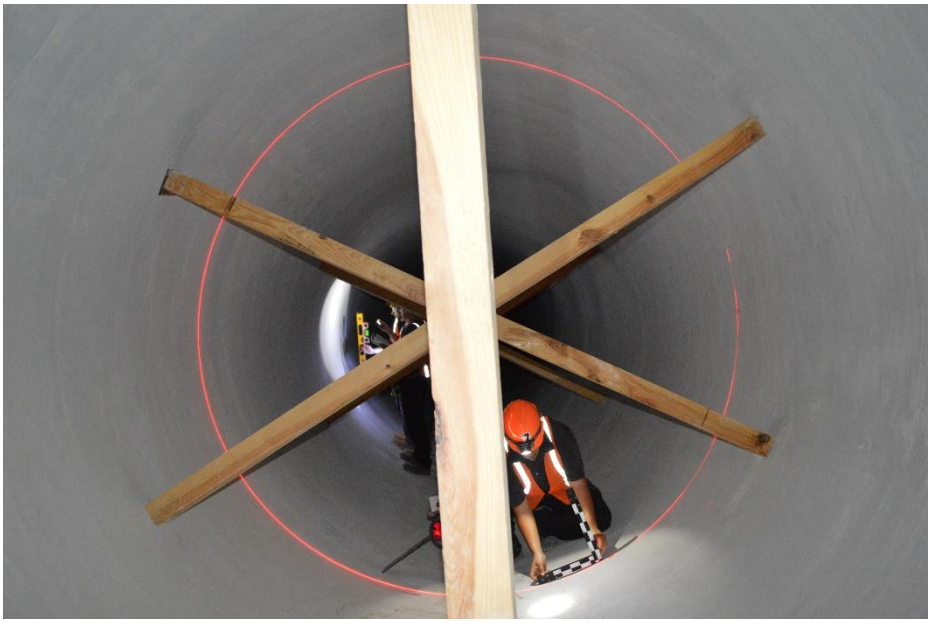

Figure 2-17 Laser photo profile method at 40ft of pipe joint number 1066 at placement

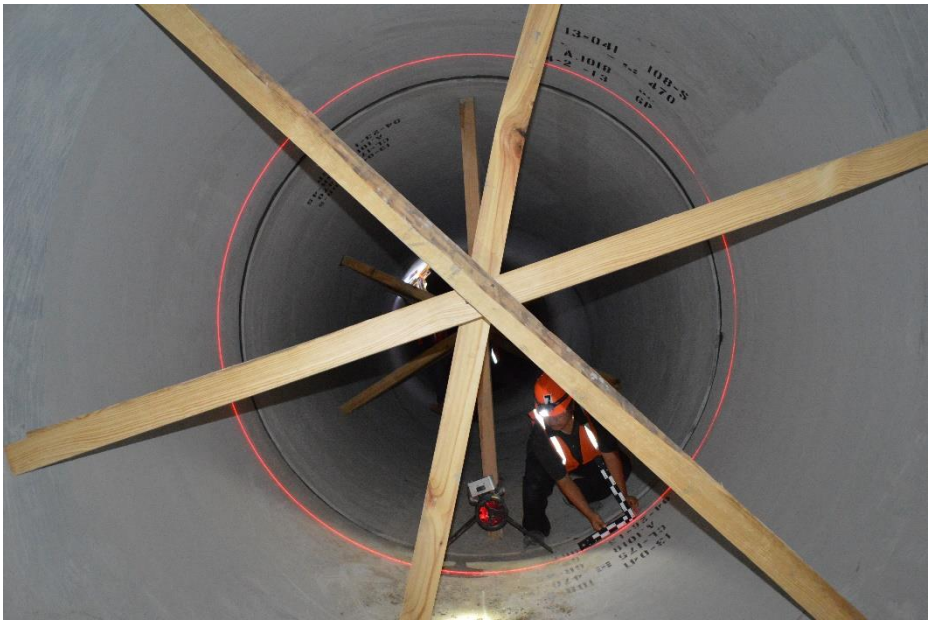

Figure 2-18 Laser photo profile method at end of pipe joint number 1066 at placement

2.4 Laser Video Profile Method

The Laser Video Profile method was used when the stulls were removed from the prove-out section and CLSM layers of 30 and 70% pipe diameter were poured and backfilled. This method was carried out in one site visit on September 13th 2013. Instrumentation for this method was comprised of data logger and console (CUES Inspector General instrumentation console), crawler with video camera (CUES rover with OZII Pan/Tilt/Zoom Camera Module (P/N CZ902)), ten-head laser ring with rechargeable battery on skid, gas generator and extension cables. Figure 2-19 shows the instrumentation for the Laser video profile method.

(a)

(c)

(b)

(d)

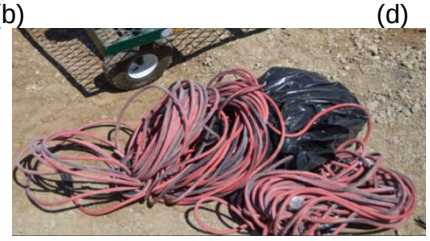

(e)

Figure 2-19 Instrumentation for the laser video profile method (a) data logger and console (b) ten-head laser ring on skid (c) crawler with video camera (d) gas generator (e) cable extension

The equipment was separated to form two (2) main sections. The data logger and console were moved to the beginning of the prove-out section, and the crawler and ten-head laser ring on skid were placed at the end of the prove-out section. Figure 2-20 shows movement of instrumentation for placement within the pipeline. Electricity from the gas generator was connected to an outlet on the data logger and console unit via power extension cords through temporary power line inlets within the pipeline. Figure 2-21 shows extension power lines via temporary power inlet holes.

Figure 2-20 Movement of instrumentation for placement within the pipeline

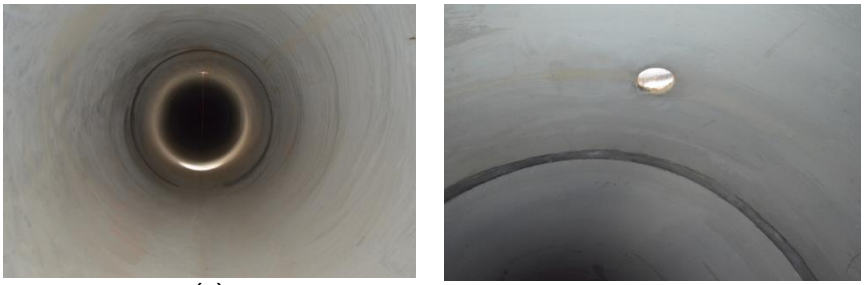

(a) (b)

Figure 2-21 Extension power lines (a) through inlet along pipeline (b) temporary power inlet hole

In the beginning of the prove-out section the data logger and console were set up and powered by an external gas generator via extension power cables. A new Digital Versatile Disk (DVD) was placed into the recording machine for each measurement. The crawler's high resolution camera was controlled via the Inspector General. The display unit of the Inspector General was monitored for CCTV footage to insure that the entire laser ring diameter was captured and displayed in the recording. Figure 2-22 shows the set-up of the data logger and console unit. The crawler was connected to the pullback cable and power extension of the data logger and console unit. The crawler was placed

in the line of symmetry of the pipeline and with the camera head facing in the direction of the skid-laser unit. The crawler was connected to the skid by a length of metal chain as shown in Figure 2-23. This length needs to be long enough for the crawler camera to be able to capture the entire circumference of the laser ring. The ten-head laser ring with the rechargeable battery was placed firmly on the skid. The skid was checked for stability and to be in line with the symmetry of the pipeline. Once the skid-laser was in placement and connected to the crawler which was connected to the data logger and console unit, forming two continuous connections, the ten-head laser ring was switched on. The laser ring covered the circumference of the pipe wall and was emitted perpendicular to the longitudinal axis of the pipe. Figure 2-24 shows the Crawler and laser-skid placement and Figure 2-25 shows the high resolution camera on the crawler.

(a) (b)

(c)

Figure 2-22 Set-up of data logger and console unit (a) data logger and console unit (b) Crawler camera and lighting control (c) Monitoring laser ring diameter from Inspector General display

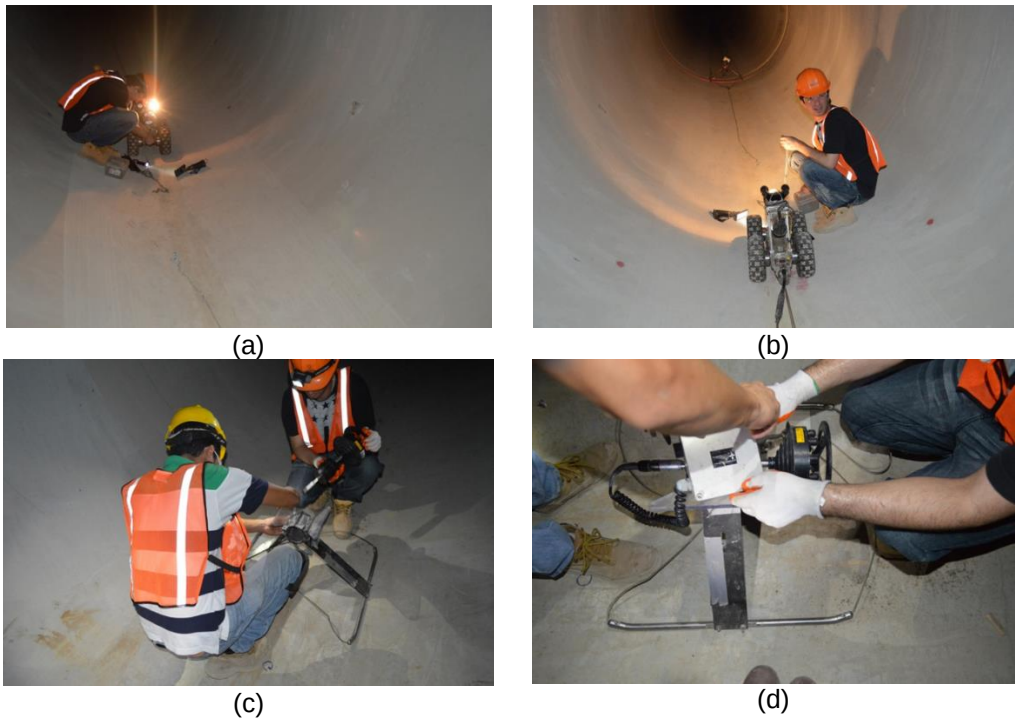

Figure 2-23 Crawler and laser-skid placement (a) Crawler to data logger cable connection (b) Crawler to laser-skid cable connection (c) ten-head laser ring placement (d) Rechargeable battery connection and placement

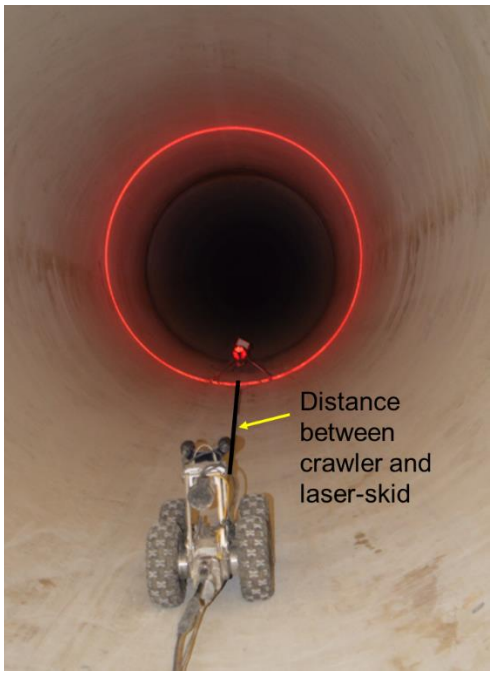

Figure 2-24 Distance required between crawler and laser-skid

Figure 2-25 High resolution camera on crawler

Before the crawler was pulled back, the entire prove-out section had to be clean from debris to avoid excessive vibration to the crawler camera to insure accurate recording of the laser-ring projection. Figure 2-26 show debris within the prove-out

section. Where possible the interference of additional light was kept to a minimum to increase the clarity of the laser ring.

(a) (b)

Figure 2-26 Debris within pipeline (a) welding joint debris (b) installation debris

When the crawler and laser-skid were set up on the other end of the prove-out section, the cable connecting the crawler was fed back at a controlled speed to capture the internal circumference of the entire prove-out section. Figure 2-27 shows the crawler being pulled back by data logger and console connecting cable. The recording was stopped and the DVD finalized once the crawler and skid-laser units were fed back across the entire prove-out section reaching the data logger and console unit. The results were then post processed using software provided with the laser profiling unit.

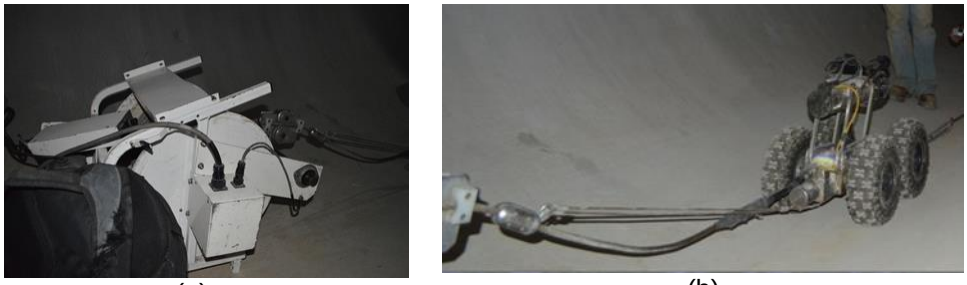

(a) (b)

Figure 2-27 Crawler being pulled back by data logger and console connecting cable (a) data logger and console connecting cable (b) crawler pulled back

Rod and laser distance meter measurements were used to verify the measurements obtained from the Laser Video Profile method at specific points along the pipeline. Figure 2-28 shows pipe horizontal and vertical diameter check via rod and Figure 2-29 shows pipe diameter check via laser distance meter.

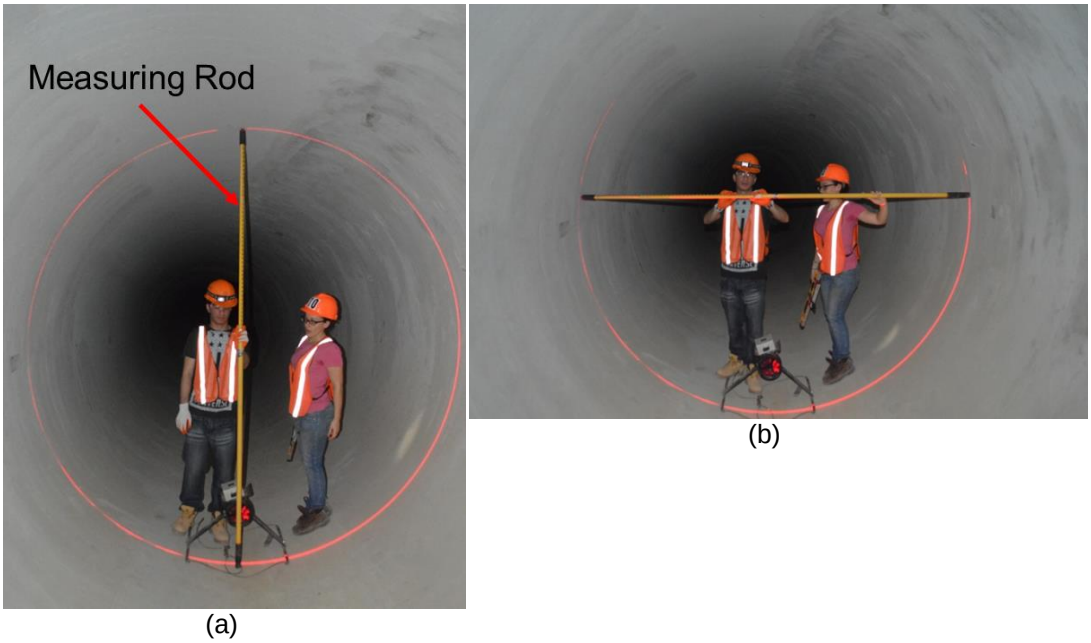

(a) (b)

Figure 2-28 Pipe diameter check via rod (a) vertical deflection (b) horizontal deflection

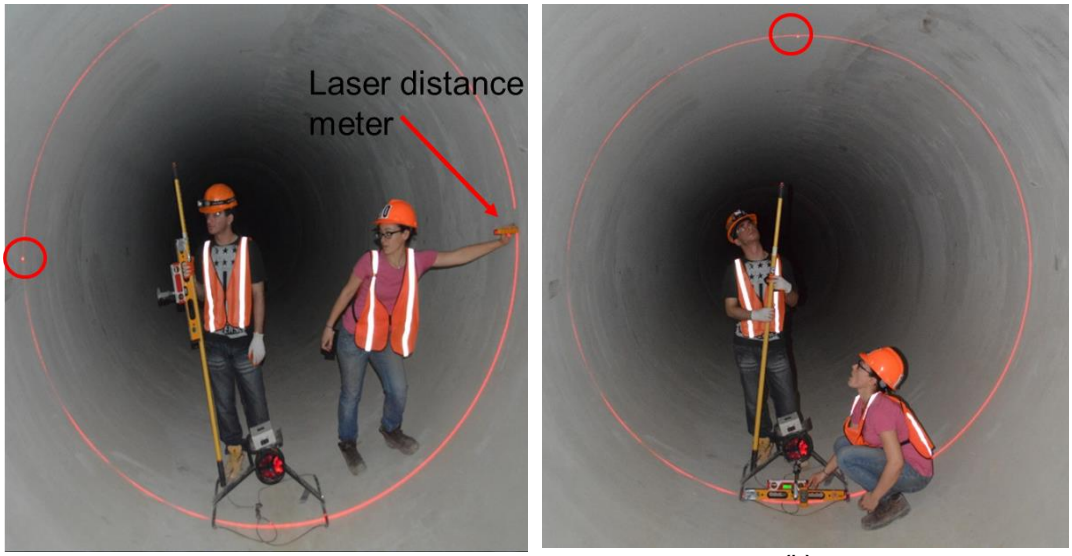

(a) (b)

Figure 2-29 Pipe diameter check via laser distance meter (a) horizontal deflection (b) vertical deflection

2.5 Field Test Results

For the MOP-119 method, after the middle ordinate (e) was obtained, the radius of curvature of the deflected pipe per section was calculated by using Equation 1.9. The larger middle ordinate value between the 90 and 45 degrees per section were used in the equation in order to obtain the maximum deflection. The graph from Figure 1-11 was used to estimate the maximum deflection in the pipe, where the maximum radii (Rmax) was obtained from Equation 1.9 and the value of circular radii was fixed at 54 inch (1.37 meter). The estimated maximum deflection obtained from the graph was recorded for each section of installation phase. Figure 2-30 shows the percent deflection obtained from the MOP-119 method for each section of the installation phase. The results obtained do not meet the AWWA deflection limit of 2%. The average maximum percent change is 2.6% at 70% CLSM installation phase. Table 2-4 shows each installation phase and the percent average change in pipe diameter.

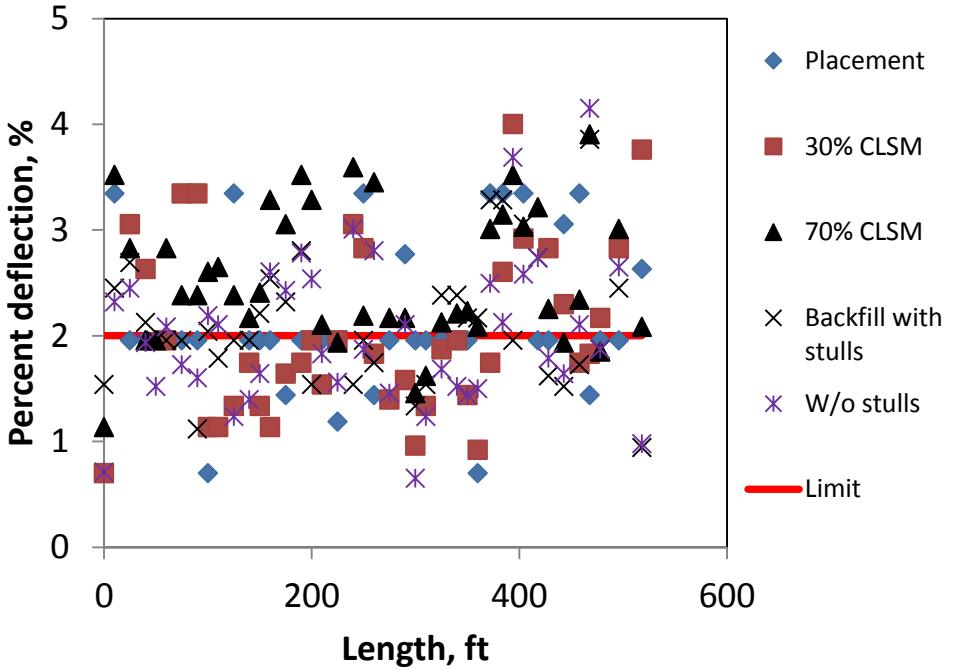

Figure 2-30 Percent deflection obtained from the MOP-119 method for each section of installation phase

Table 2-4 Percent average change in pipe diameter per installation phase

Installation phase	Average pipe diameter change (%)
Placement	2.3
30% CLSM	2.2
70% CLSM	2.6
Backfill (stulls)	2.2
Backfill (w/o stulls)	2.1

For the Laser Photo Profile method, the pictures taken were imported to AUTOCAD 2011 software and processed to measure the horizontal and vertical deflection. A scale of known length, which was seen in all the pictures, was used to

convert picture length to actual length. Figure 2-31 shows the post photo processing in AUTOCAD 2011 to measure deflection.

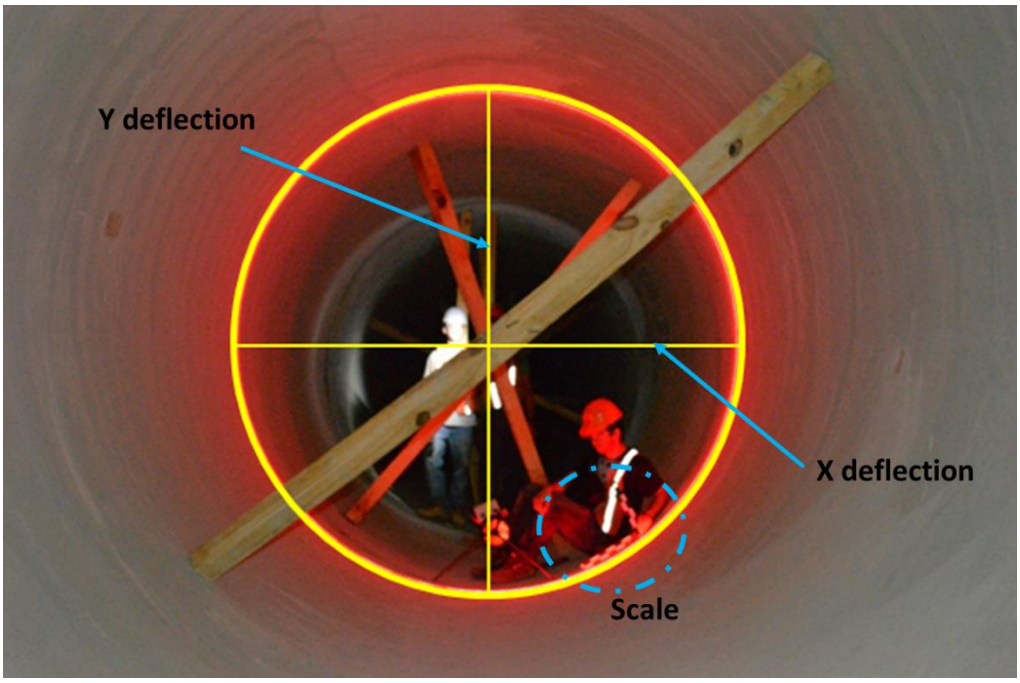

Figure 2-31 Photo processing in AUTOCAD 2011 to measure deflection

The X and Y deflection measurements obtained from AUTOCAD software for each installation phase section was recorded against the initial pipe diameter. Figure 2-32 shows the change in the horizontal diameter of the pipeline with respect to the original pipe diameter in each installation phase. Figure 2-33 shows the change in the vertical diameter of the pipeline with respect to the original pipe diameter in each installation phase. The results obtained from the Laser Photo Profile method are by and large within the 2% limit for deflection as per AWWA standard.

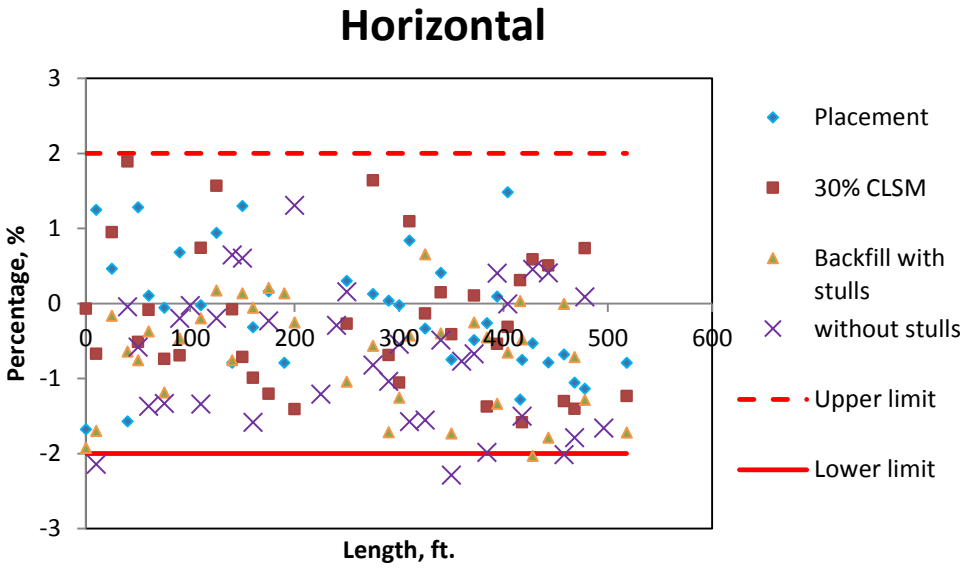

Figure 2-32 Change in the horizontal diameter of the pipeline with respect to the original pipe diameter in each installation phase

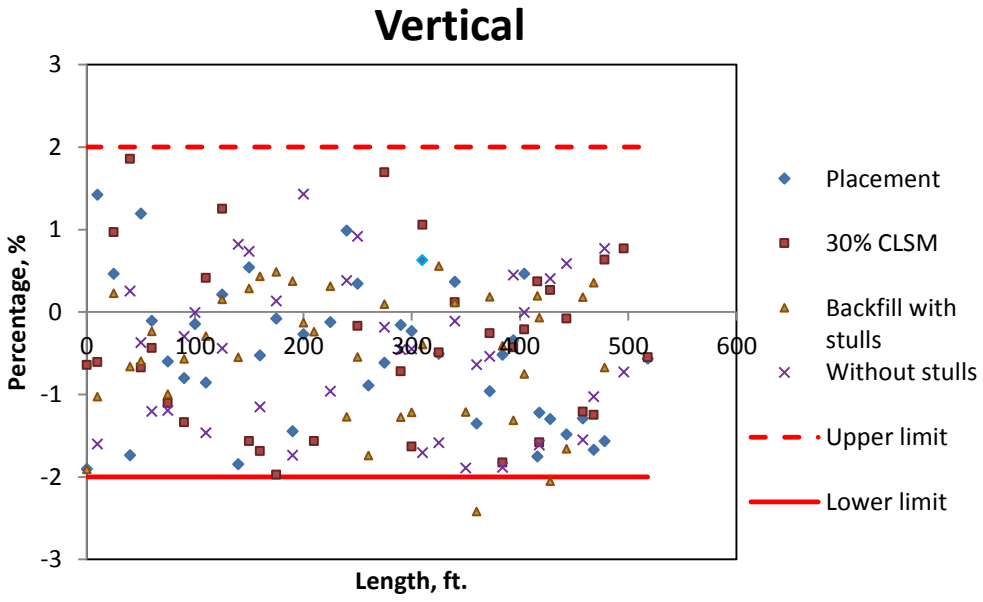

Figure 2-33 Change in the vertical diameter of the pipeline with respect to the original pipe diameter in each installation phase

For the Laser Video Profile method, the finalized data from the DVD was post processed using software provided with the laser profiling unit. The change in the pipe diameter, in vertical and horizontal directions or the deformation of the pipeline, was calculated as a percentage change from the initial internal diameter. Ovality was calculated by Equation 1.10 and the mean inside diameter was obtained from profiler software. A typical view of the profiler software is shown in Figure 2-34, and Figure 2-35 shows profiler software analyzing a deformed ring and an un-deformed ring taken from a single frame from a sample video recording not taken from the prove-out section.

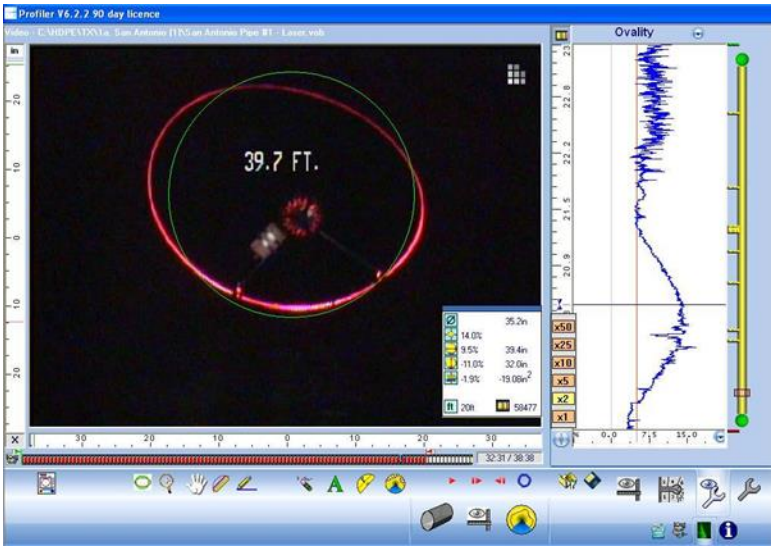

Figure 2-34 Typical view of the profiler software

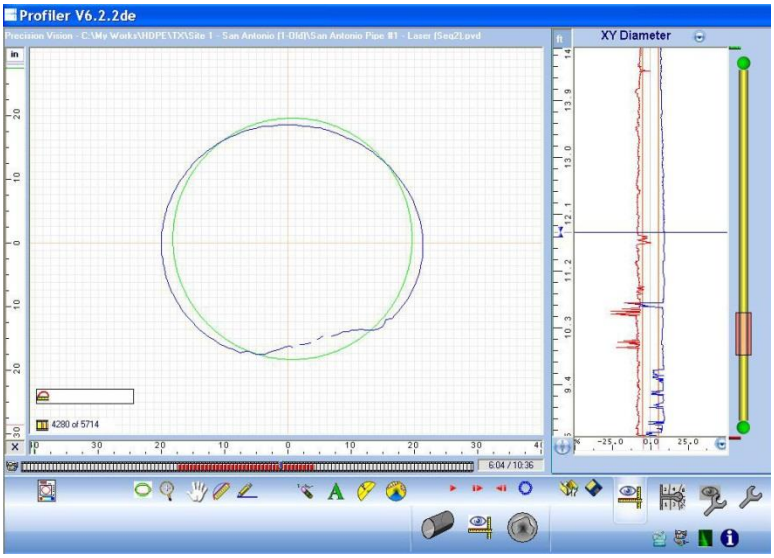

Figure 2-35 Profiler software analyzing a deformed ring and an un-deformed ring taken from a single frame from a sample video recording

The profiler software provided the maximum and minimum deflection values at each section of the prove-out. The maximum deflection value is any point in the circumference of the pipe wall where the change in pipe diameter compared to the original diameter is positive (greater than 108 inch). Similarly, the minimum deflection value is the point in the circumference of the pipe wall where the change in pipe diameter compared to the original diameter is negative (less than 108 inch). The horizontal and vertical deflections, along with the maximum and minimum deflections, were all within the 2% deflection limit as per AWWA specifications. Figure 2-36 shows the percent of change in the vertical and horizontal diameter across the prove-out section by the Laser Video Profile method. Figure 2-37 shows the maximum and Figure 2-38 the minimum percent change in deflection across prove-out section. The rod and laser measurements were used to verify the accuracy of scales used in the measuring methods. The Laser Video Profile method results were within close range to the rod and laser meter readings.

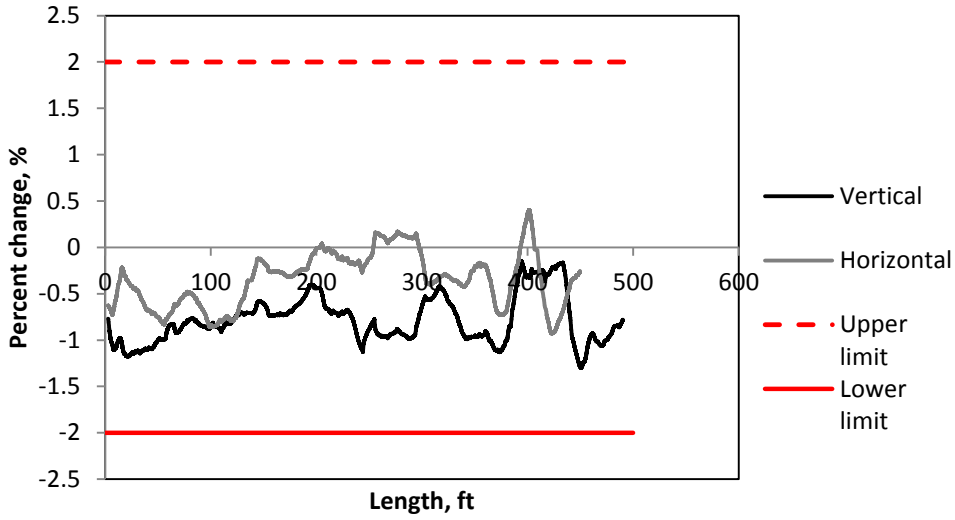

Figure 2-36 Percent change in the vertical and horizontal diameter across the prove-out section by Laser Video Profile method

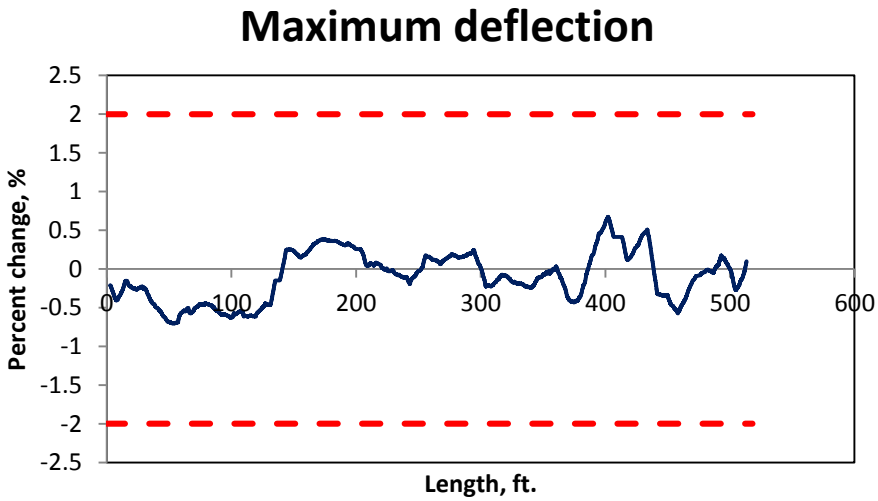

Figure 2-37 Percent change in the maximum deflection across the prove-out section by Laser Video Profile method

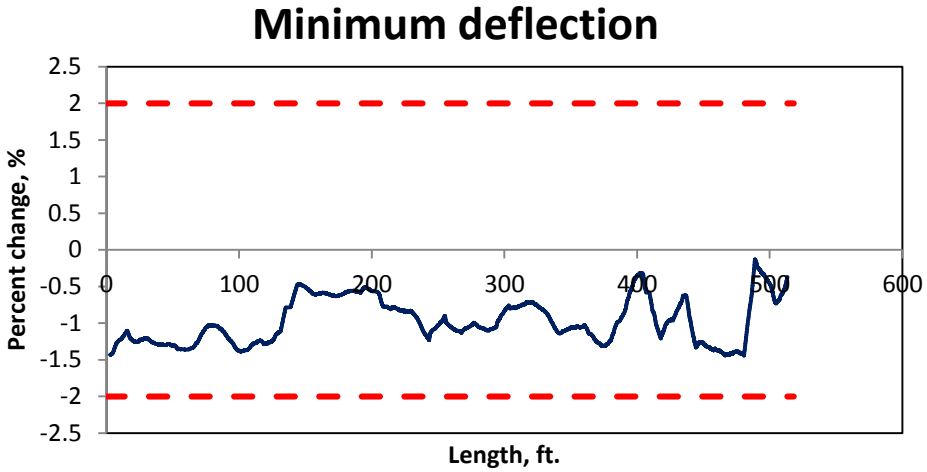

Figure 2-38 Percent change in the minimum deflection across the prove-out section by Laser Video Profile method

2.6 CLSM Material Testing

The CLSM used in the prove-out section did not contain any fly-ash. The CLSM was poured into two (2) lifts to avoid pipe floatation. The first lift was poured to 30% pipe diameter and the second to 70%. The CLSM was produced on-site with a travelling batch plant, as shown in Figure 2-39. The CLSM used for casting beams and cylinders were taken from a sample, as per ASTM D 5971-07, of CLSM produced by the automated travelling batch plant, as shown in Figure 2-40.

Figure 2-39 Travelling batch plant

Figure 2-40 Sample CLSM produced by the automated travelling batch plant

2.6.1 CLSM Casting

Beam and cylinder casting were produced on-site as per Standard Practice for Making and Curing Concrete Test Specimens in the Field (ASTM C31/C31M-12). Beams were casted into molds of 20in. (508mm) in length, 6in. (152mm) in height and width. Cylinders were produced into plastic molds of 4in. (101.6mm) in diameter and 12in. (304.8mm) in height. Ten (10) beams and cylinders were casted. No compaction or vibration table was needed, as CLSM is self-leveling. The molds were filled with CLSM

and the top surface smoothed for a flat surface. The Molds were covered with a plastic sheet to harden and cure at the site for 21 days. Figure 2-41 shows the casting procedure of the CLSM beam and cylinder molds.

(a) (b)

(c) (d)

Figure 2-41 Casting procedure of CLSM beam and cylinder molds (a) pouring CLSM in mold (b) Filling mold with CLSM (c) Leveling surface for smoothness (d) Molds set for curing

2.6.2 CLSM Testing

Beam and cylinder molds were tested as per Standard Test Method for Flexural Strength of Concrete (ASTM C78/C78M-10) and Standard Test Method for Preparation and Testing of Controlled Low Strength Material Test Cylinders (ASTM D 4832-10). Tests were carried out in the University of Texas at Arlington Civil Engineering Lab Building (CELB) after twenty-one (21) days of curing. The CLSM specimens were removed from

the beam and cylinder molds for testing. Some of the CLSM specimens got damaged during removal. Four (4) beam specimens were tested successfully for flexure and three (3) cylinder specimens for compression strength. The beams were tested by using the Material Testing Systems (MTS) machine as shown in Figure 2-42.

(a) (b)

Figure 2-42 CLSM specimen beam flexure test by MTS machine (a) test set-up (b) after failure

Prior to testing the CLSM cylinder specimens for compression, the specimens top and bottom surfaces were capped with flake capping sulfur compound. Silica chips were heated to liquid form and placed into a cap mold where the specimen surface was pressed upon the liquid hardening. This procedure was carried out to make both surfaces parallel and smooth to insure uniform loading when placed in the Compressive Cylinder Testing machine. The capping via sulfur proved difficult for the CLSM specimens as they broke easily during removal of sulfur cap mold as shown in Figure 2-43. Only one (1) specimen was capped successfully with sulfur and the other two (2) were tested without capping but with a smooth surface applied with a hard brush. The surface of the load plate was cleaned after each test to prevent uneven loading on the specimens. The

loading rate was applied as per standard, continuously and without shock. The load was applied until the specimen failed as shown in Figure 2-44. The maximum load carried by the specimen was recorded.

(a) (b)

Figure 2-43 Capping of specimen (a) Sulfur capping (b) Specimen damaged during sulfur capping

Figure 2-44 Specimen failure

2.6.3 Results

The result of the CLSM compressive test is shown in Table 2-5 below. Three (3) specimens were successfully tested, two (2) uncapped and one (1) sulfur capped. The ultimate load carried by each specimen was recorded. The compressive strength (stress) of each specimen was also calculated based on Equation 2.1. The ratio of peak load to compressive strength for the specimens averaged to a value of 12.5.

$$C = \frac{L}{\pi(D^2)/4} \quad (2.1)$$

Where,

C = compressive strength, lbf/in.2 (kPa)

D = nominal diameter of cylinder, 4in. (101.6 mm)

L = maximum load, lbf (kN)

Table 2-5 Compressive strength test results

Specimen	Peak Load	Compressive strength
Uncapped	740 lb. (3292 N)	58.89 psi (406 kPa)
Uncapped	630 lb. (2802 N)	50.13 psi (345.6 kPa)
Capped (sulfur)	1620 lb. (7206 N)	128.92 psi (888.8 kPa)

The flexural beam tests produced load-deflection graphs from the average deflection values obtained from the two Linear Variable Displacement Transducers (LVDTs). The Load deflection graph displays the first peak load and ultimate load. Figure 2-45 shows the load-deflection graph for the four (4) CLSM beam flexure specimens. It can be observed that the peak-load value ranged between 30 to 60 lb. (133.5 to 267 N) and the maximum displacement before failure ranged from 0.01 to 0.04 in. (0.25 to 1.0 mm).

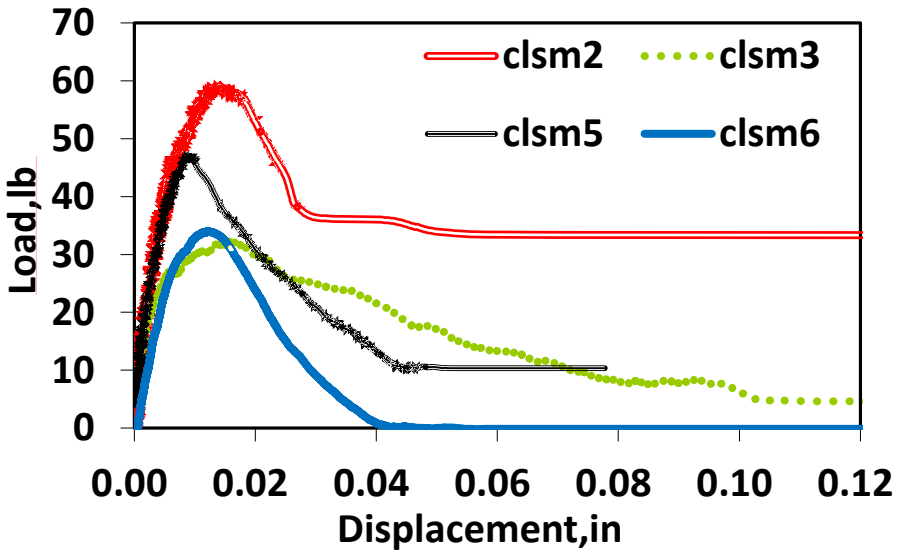

Figure 2-45 Load-deflection graph for the 4 CLSM specimens

Chapter 3

Summary, Conclusion and Recommendation

3.1 Summary

The main aim of this study was to compare deflection measurement methods for 108 inch steel pipes with mortar lining embedded with CLSM. Field tests were carried out in the prove-out section of line J of IPL. The prove-out is a section of line J that was used for experimental research for the use of CLSM as an embedment material and for calibrating the FEM model for the rest of the pipeline. The prove-out section was comprised of 11 pipes, varying in length from 24 ft. to 50 ft. (7.3-15.2 m), with a total length of 518 ft. (157.8 m). Three (3) methods were used to measure pipe deflection: MOP-119, Laser Photo Profile and Laser Video Profile. The MOP-119 method was compared to the Laser Photo Profile method when the stulls were present in the pipeline and later with both the Laser Photo and Video Profile method when the stulls were removed. The schedule for deflection measurements was based on the progress of construction of the different phases of pipe installation. There were forty-three (43) sections in the prove-out where measurements were taken with the MOP-119 and Laser Photo Profile method. The Laser Video Profile method was run continuously through the entire length of the prove-out section without any breaks.

The structural integrity of the installed steel pipes was monitored by comparing the deflection measurements obtained from the three methods to the recommended deflection limit of 2% pipe diameter set by the American Water Works Association (AWWA M11).

The use of CLSM as an embedment material was also studied in this research. Beam and cylinder specimens were produced on-site as per ASTM C31/C31M-12. Beams were casted into molds of 20 in. (508 mm) in length, 6 in. (152 mm) in height and

width. Cylinders were produced into plastic molds of 4 in. (101.6 mm) in diameter and 12 in. (304.8mm) in height. Ten (10) beams and cylinders were casted. Beam and cylinder molds were tested as per ASTM C78/C78M-10 and ASTM D 4832-10. Testing was carried out in the University of Texas at Arlington Civil Engineering Lab Building (CELB) after twenty-one (21) days of curing. Four (4) beam specimens were successfully tested for flexure and three (3) cylinder specimens for compression strength.

3.2 Conclusion

Experimental field tests were carried out to measure pipe deflection at various installation phases. The three (3) methods used to measure deflection were successfully conducted along the prove-out section of the pipeline. The MOP-119 method produced percent deflection to initial pipe diameter values more than the set limit of 2% as per AWWA specification. The average maximum percent change in pipe diameter was 2.6% at 70% installation phase. The Laser Photo Profile and Laser Video Profile method both produced readings within the 2% limit.

The MOP-119 is based on theoretical analysis of a buried pipe in a homogeneous, isotropic, elastic medium, ASCE Buried Flexible Steel Pipe (2009). This was not the condition for the prove-out section pipeline. This method is more susceptible to human error and judgment than the Laser Video Profile method. The Laser Video Profile method is more realistic, as it is performed on-site and real data are post-processed rather than estimating results by graph.

The use of CLSM as an embedment material was also concluded to be satisfactory. The installed pipeline used a narrow trench as compared to compacted soil backfill, and there was no need for compaction equipment, which reduced the cost of trench excavation. The post-installation deflection checks, within the 2% AWWA limit based on the Laser Photo and Video profile methods, showed that CLSM was able to

form a composite system with the pipe to carry the loads that cause excessive deflection and buckling. The average twenty-one (21) day compressive strength of CLSM cylinder samples was 78.6 psi (0.54Mpa) as per ASTM D 4832-10 specifications and fall within ACI 116R-00 recommended range of less than 1200 psi (8.27 MPa).

3.3 Recommendation

The recommendations for future studies are:

1. Continue deflection measurements for the rest of the Line J pipeline by using the Laser Photo Profile method while stulls are present in the pipeline and the Laser Video Profile method when the pipeline is clear from stulls and debris.
2. Re-visit the prove-out section to measure deflection measurements after the pipeline has been pressurized and monitor crack patterns for large cracks greater than 1/16 inch width (1.58 mm) and small cracks for autogenous healing in moist environment.
3. Model Prove-out section and CLSM with Finite Element Method (FEM).

Appendix A

MOP-119 method for middle ordinate values at 90 degrees

			Level profiling 90deg					
				1	2	3	4	
	Pipe#	Section #	Distance	Placement	30% CLSM	70% CLSM	Full backfill	
50 ft	**66**	**Joint**	0ft	1.50	1.44	1.30	1.36	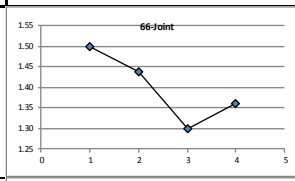
	//	10ft	10ft	1.19	1.25	1.18	1.23	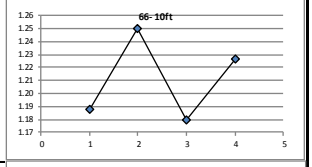
	//	25ft	25ft	1.31	1.25	1.21	1.22	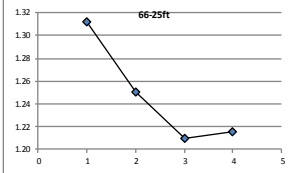
	//	40ft	40ft	1.25	1.22	1.25	1.24	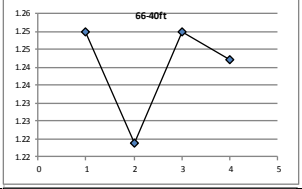
	67	**Joint**	50ft	1.26	1.28	1.26	1.31	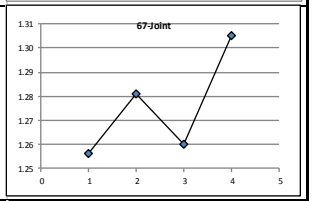

Figure A-1 Comparison of middle ordinate values (e) obtained at 90 degrees from MOP-119 method for all installation phases of pipe no.66

	Pipe#	Section #	Distance	Placement	30% CLSM	70% CLSM	Full backfill	
50ft	67	10ft	60ft	1.25	1.25	1.21	1.25	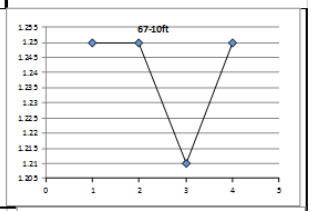
	//	25ft	75ft	1.32	1.28	1.23	1.25	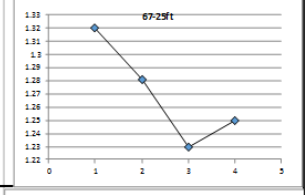
	//	40ft	90ft	1.25	1.26	1.23	1.29	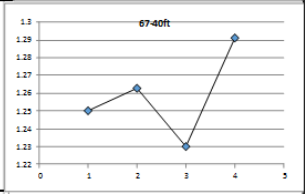
	68	**Joint**	100ft	1.31	1.29	1.22	1.25	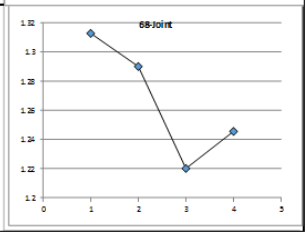

Figure A-2 Comparison of middle ordinate values (e) obtained at 90 degrees from MOP-119 method for all installation phases of pipe no.67

				Level profiling 90deg				
				1	2	3	4	
	Pipe#	Section #	Distance	Placement	30% CLSM	70% CLSM	Full backfill	
50ft	68	10ft	110ft	1.31	1.29	1.22	1.26	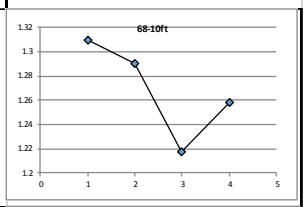
	//	25ft	125ft	1.31	1.28	1.26	1.28	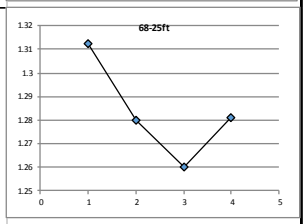
	//	40ft	140ft	1.31	1.32	1.25	1.27	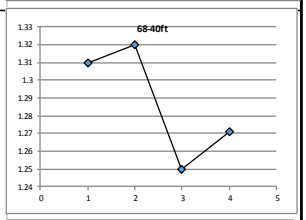
	69	**Joint**	150ft	1.31	1.30	1.23	1.24	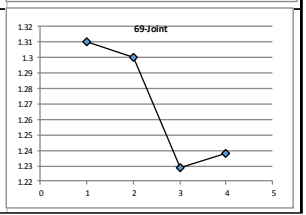

Figure A-3 Comparison of middle ordinate values (e) obtained at 90 degrees from MOP-119 method for all installation phases of pipe no.68

			Level profiling 90deg					
				1	2	3	4	
	Pipe#	Section #	Distance	Placement	30% CLSM	70% CLSM	Full backfill	
50ft	//	10ft	160ft	1.25	1.29	1.19	1.22	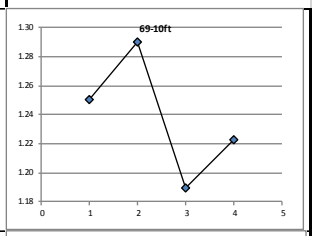
	//	25ft	175ft	1.28	1.27	1.20	1.23	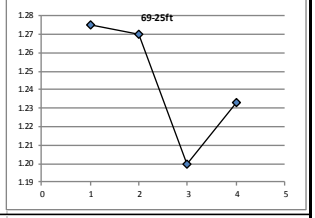
	//	40ft	190ft	1.25	1.26	1.18	1.21	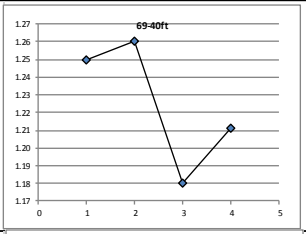
	70	**Joint**	200ft	1.25	1.27	1.19	1.35	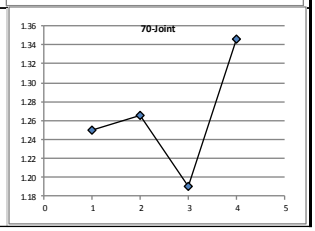

Figure A-4 Comparison of middle ordinate values (e) obtained at 90 degrees from MOP-119 method for all installation phases of pipe no.69

			Level profiling 90deg					
				1	2	3	4	
	Pipe#	Section #	Distance	Placement	30% CLSM	70% CLSM	Full backfill	
50ft	70	10ft	210ft	1.29	1.27	1.24	1.38	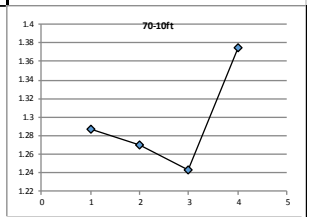
	//	25ft	225ft	1.31	1.27	1.25	1.40	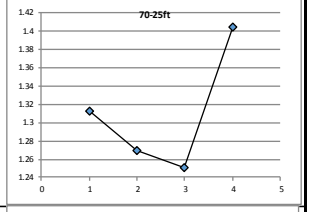
	//	40ft	240ft	1.20	1.20	1.18	1.32	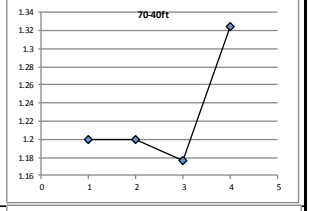
	71	**Joint**	250ft	1.35	1.30	1.24	1.32	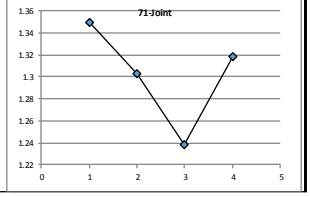

Figure A-5 Comparison of middle ordinate values (e) obtained at 90 degrees from MOP-119 method for all installation phases of pipe no.70

				Level profiling 90deg				
				1	2	3	4	
	Pipe#	Section #	Distance	Placement	30% CLSM	70% CLSM	Full backfill	
50ft	71	10ft	260ft	1.31	1.26	1.18	1.33	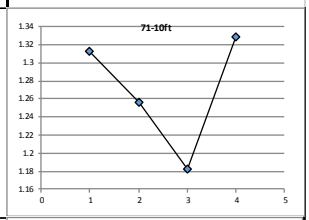
	//	25ft	275ft	1.25	1.28	1.24	1.38	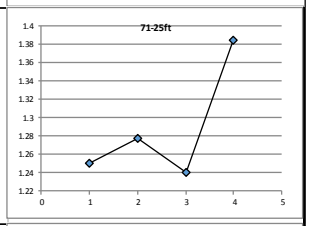
	//	40ft	290ft	1.25	1.27	1.24	1.45	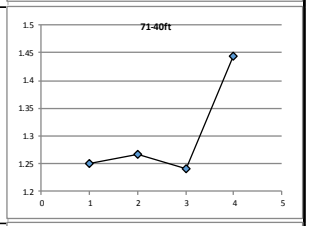
	72	**Joint**	300ft	1.25	1.30	1.28	1.28	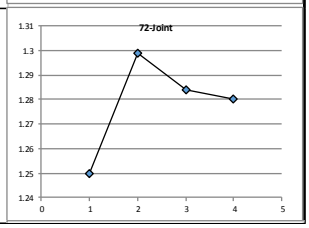

Figure A-6 Comparison of middle ordinate values (e) obtained at 90 degrees from MOP-119 method for all installation phases of pipe no.71

			Level profiling 90deg					
				1	2	3	4	
	Pipe#	Section #	Distance	Placement	30% CLSM	70% CLSM	Full backfill	
50ft	72	10ft	310ft	1.31	1.28	1.27	1.27	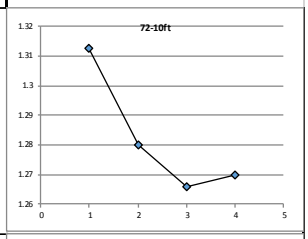
	//	25ft	325ft	1.25	1.25	1.24	1.23	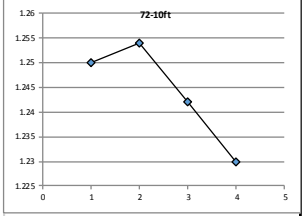
	//	40ft	340ft	1.25	1.25	1.24	1.23	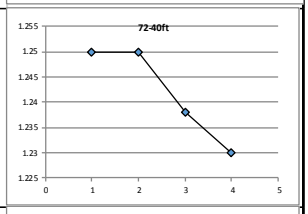
	73	**Joint**	350ft	1.25	1.28	1.24	1.24	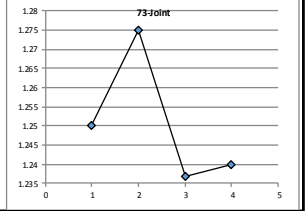

Figure A-7 Comparison of middle ordinate values (e) obtained at 90 degrees from MOP-119 method for all installation phases of pipe no.72

			Level profiling 90deg					
				1	2	3	4	
	Pipe#	Section #	Distance	Placement	30% CLSM	70% CLSM	Full backfill	
44ft	73	10ft	360ft	1.31	1.31	1.25	1.24	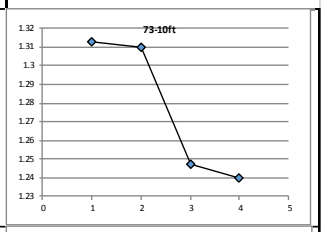
	//	22ft	372ft	1.33	1.26	1.20	1.19	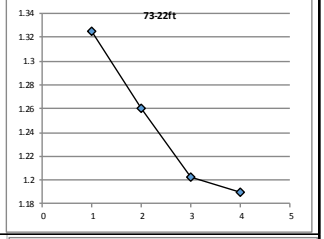
	//	34ft	384ft	1.25	1.22	1.20	1.19	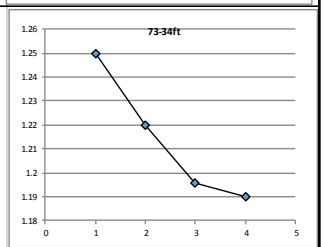
	74	**Joint**	394ft	1.23	1.29	1.26	1.27	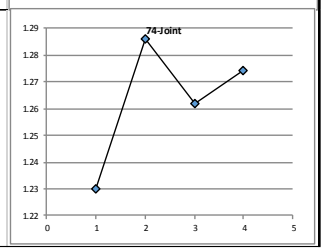

Figure A-8 Comparison of middle ordinate values (e) obtained at 90 degrees from MOP-119 method for all installation phases of pipe no.73

				Level profiling 90deg				
				1	2	3	4	
	Pipe#	Section #	Distance	Placement	30% CLSM	70% CLSM	Full backfill	
24ft	74	10ft	404ft	1.38	1.22	1.23	1.23	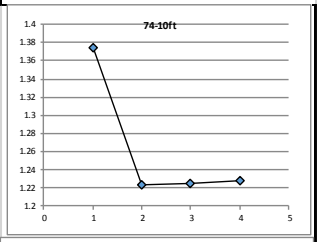
	//	22ft	416ft	1.13	1.12	1.12	1.13	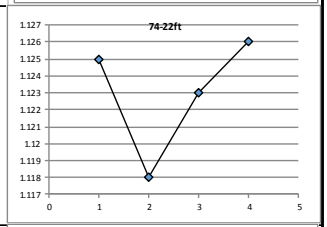
	75	**Joint**	418ft	1.25	1.14	1.19	1.21	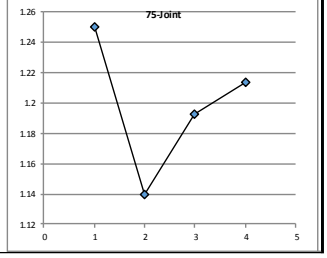

Figure A-9 Comparison of middle ordinate values (e) obtained at 90 degrees from MOP-119 method for all installation phases of pipe no.74

			Level profiling 90deg					
				1	2	3	4	
	Pipe#	Section #	Distance	Placement	30% CLSM	70% CLSM	Full backfill	
50ft	75	10ft	428ft	1.25	1.21	1.24	1.27	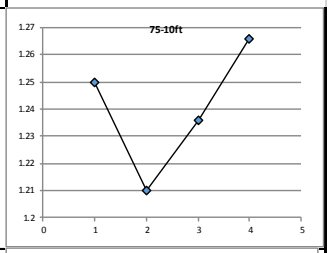
	//	25ft	443ft	1.31	1.23	1.26	1.27	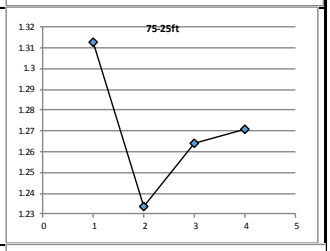
	//	40ft	458ft	1.31	1.26	1.24	1.26	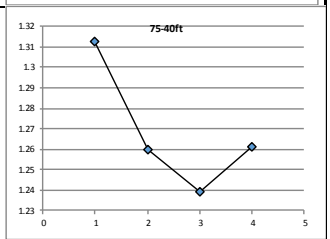
	76	**Joint**	468ft	1.28	1.26	1.22	1.25	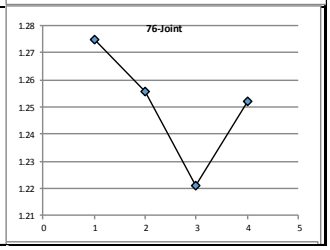

Figure A-10 Comparison of middle ordinate values (e) obtained at 90 degrees from MOP-119 method for all installation phases of pipe no.75

			Level profiling 90deg					
				1	2	3	4	
	Pipe#	Section #	Distance	Placement	30% CLSM	70% CLSM	Full backfill	
50ft	76	10ft	478ft	1.25	1.29	1.29	1.32	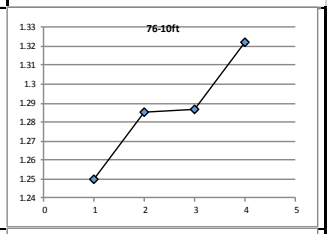
	//	28ft	496ft	1.25	1.22	1.21	1.23	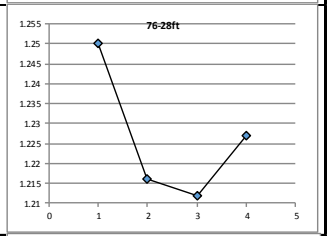
	END	**Joint**	518ft	1.25	1.30	1.33	1.31	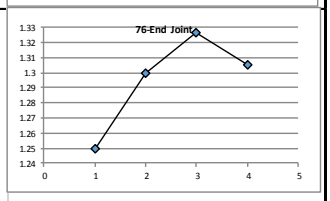
Total	11 pipes							

Figure A-11 Comparison of middle ordinate values (e) obtained at 90 degrees from MOP-119 method for all installation phases of pipe no.76

Appendix B

MOP-119 method for middle ordinate values at 45 degrees

			Level profiling 45deg					
				1	2	3	4	
	Pipe#	Section #	Distance	Placement	30% CLSM	70% CLSM	Full backfill	
50 ft	**66**	**Joint**	0ft	1.31	1.3125	1.29	1.285	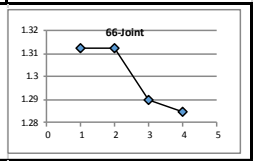
	//	10ft	10ft	1.25	0.21875	1.31	1.297	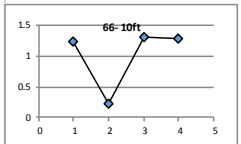
	//	25ft	25ft	1.25	1.2	1.29	1.295	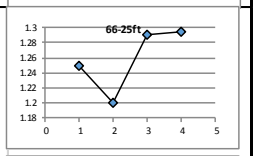
	//	40ft	40ft	1.25	1.25	1.32	1.31	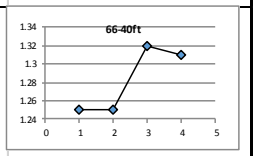
	67	**Joint**	50ft	1.25	1.1875	1.25	1.284	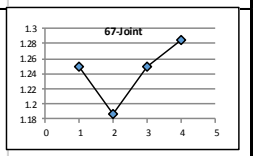

Figure B-1 Comparison of middle ordinate values (e) obtained at 45 degrees from MOP-119 method for all installation phases of pipe no.66

			Level profiling 45deg					
				1	2	3	4	
	Pipe#	Section #	Distance	Placement	30% CLSM	70% CLSM	Full backfill	
50ft	67	10ft	60ft	1.34	1.25	1.34	1.367	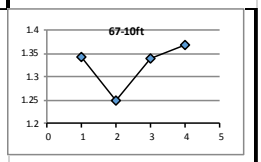
	//	25ft	75ft	1.25	1.1875	1.31	1.331	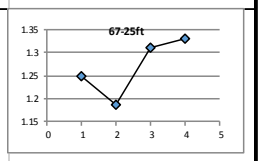
	//	40ft	90ft	1.25	1.1875	1.33	1.325	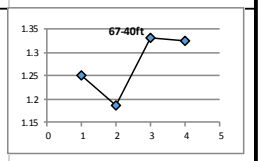
	68	**Joint**	100ft	1.31	1.32	1.27	1.291	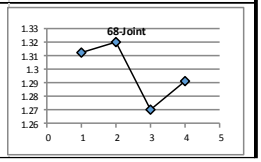

Figure B-2 Comparison of middle ordinate values (e) obtained at 45 degrees from MOP-119 method for all installation phases of pipe no.67

			Level profiling 45deg					
				1	2	3	4	
	Pipe#	Section #	Distance	Placement	30% CLSM	70% CLSM	Full backfill	
50ft	68	10ft	110ft	1.13	1.32	1.24	1.276	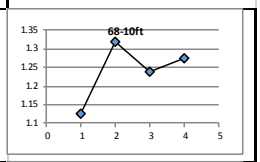
	//	25ft	125ft	1.19	1.307	1.23	1.252	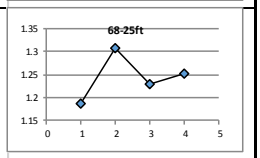
	//	40ft	140ft	1.25	1.26	1.24	1.278	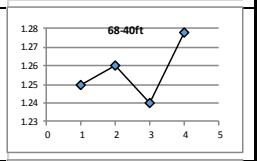
	69	**Joint**	150ft	1.25	1.28	1.32	1.333	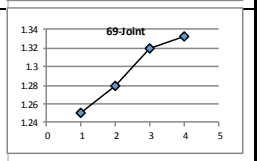

Figure B-3 Comparison of middle ordinate values (e) obtained at 45 degrees from MOP-119 method for all installation phases of pipe no.68

			Level profiling 45deg					
				1	2	3	4	
	Pipe#	Section #	Distance	Placement	30% CLSM	70% CLSM	Full backfill	
50ft	69	10ft	160ft	1.29	1.29	1.32	1.341	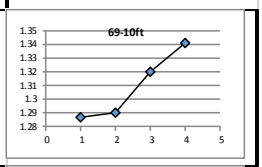
	//	25ft	175ft	1.29	1.265	1.292	1.3	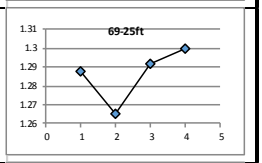
	//	40ft	190ft	1.29	1.28	1.318	1.326	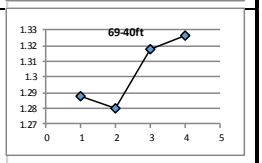
	70	**Joint**	200ft	1.25	1.25	1.238	1.416	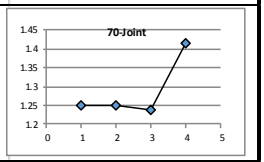

Figure B-4 Comparison of middle ordinate values (e) obtained at 45 degrees from MOP-119 method for all installation phases of pipe no.69

			Level profiling 45deg					
				1	2	3	4	
	Pipe#	Section #	Distance	Placement	30% CLSM	70% CLSM	Full backfill	
50ft	70	10ft	210ft	1.25	1.27	1.275	1.425	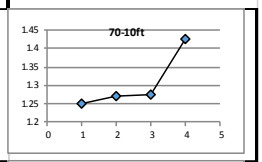
	//	25ft	225ft	1.29	1.25	1.251	1.403	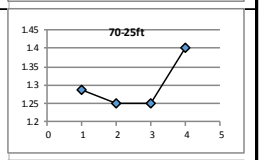
	//	40ft	240ft	1.28	1.248	1.266	1.399	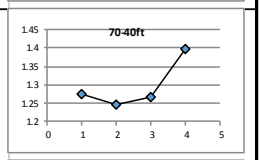
	71	**Joint**	250ft	1.19	1.21	1.258	1.393	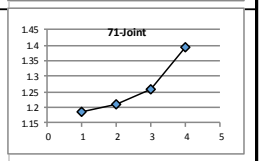

Figure B-5 Comparison of middle ordinate values (e) obtained at 45 degrees from MOP-119 method for all installation phases of pipe no.70

			Level profiling 45deg					
				1	2	3	4	
	Pipe#	Section #	Distance	Placement	30% CLSM	70% CLSM	Full backfill	
50ft	71	10ft	260ft	1.28	1.26	1.295	1.416	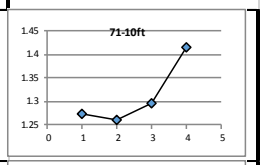
	//	25ft	275ft	1.28	1.278	1.287	1.4	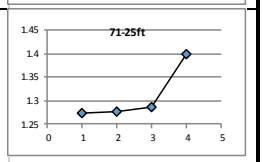
	//	40ft	290ft	1.21	1.282	1.27	1.4211	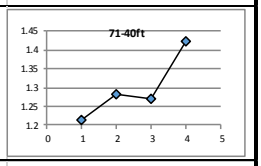
	72	**Joint**	300ft	1.25	1.32	1.274	1.28	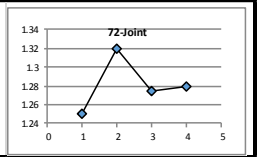

Figure B-6 Comparison of middle ordinate values (e) obtained at 45 degrees from MOP-119 method for all installation phases of pipe no.71

			Level profiling 45deg					
				1	2	3	4	
	Pipe#	Section #	Distance	Placement	30% CLSM	70% CLSM	Full backfill	
50ft	72	10ft	310ft	1.25	1.3	1.276	1.27	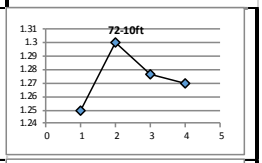
	//	25ft	325ft	1.25	1.32	1.286	1.28	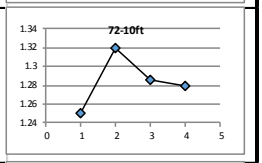
	//	40ft	340ft	1.25	1.327	1.287	1.29	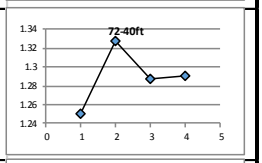
	73	**Joint**	350ft	1.3625	1.296	1.263	1.28	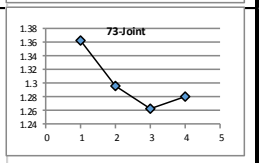

Figure B-7 Comparison of middle ordinate values (e) obtained at 45 degrees from MOP-119 method for all installation phases of pipe no.72

			Level profiling 45deg					
				1	2	3	4	
	Pipe#	Section #	Distance	Placement	30% CLSM	70% CLSM	Full backfill	
44ft	73	10ft	360ft	1.3125	1.301	1.244	1.25	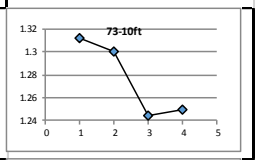
	//	22ft	372ft	1.1875	1.302	1.274	1.25	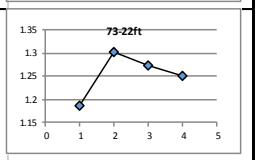
	//	34ft	384ft	1.1875	1.28	1.27	1.28	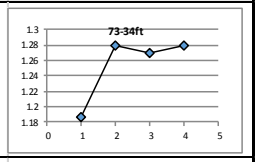
	74	**Joint**	394ft	1.125	1.16	1.18	1.195	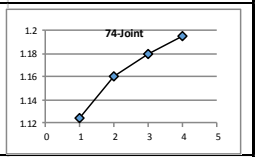

Figure B-8 Comparison of middle ordinate values (e) obtained at 45 degrees from MOP-119 method for all installation phases of pipe no.73

			Level profiling 45deg					
				1	2	3	4	
	Pipe#	Section #	Distance	Placement	30% CLSM	70% CLSM	Full backfill	
24ft	74	10ft	404ft	1.1875	1.206	1.201	1.245	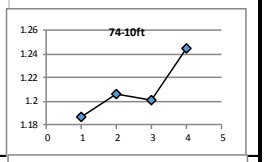
	//	22ft	416ft	1.21875	1.07	1.1	1.086	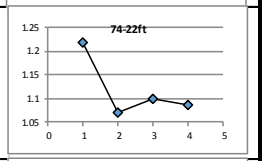
	75	**Joint**	418ft	1.375	1.286	1.269	1.33	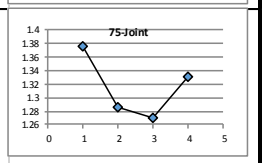

Figure B-9 Comparison of middle ordinate values (e) obtained at 45 degrees from MOP-119 method for all installation phases of pipe no.74

			Level profiling 45deg					
				1	2	3	4	
	Pipe#	Section #	Distance	Placement	30% CLSM	70% CLSM	Full backfill	
50ft	75	10ft	428ft	1.25	1.26	1.258	1.281	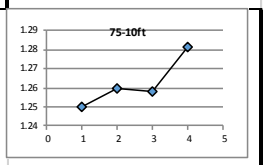
	//	25ft	443ft	1.2	1.276	1.251	1.291	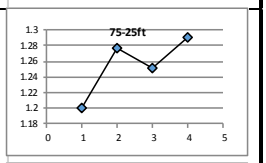
	//	40ft	458ft	1.1875	1.262	1.232	1.276	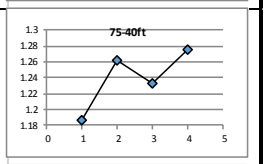
	76	**Joint**	468ft	1.28125	1.41	1.164	1.166	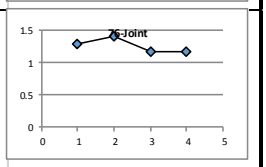

Figure B-10 Comparison of middle ordinate values (e) obtained at 45 degrees from MOP-119 method for all installation phases of pipe no.75

			Level profiling 45deg					
				1	2	3	4	
	Pipe#	Section #	Distance	Placement	30% CLSM	70% CLSM	Full backfill	
50ft	76	10ft	478ft	1.25	1.24	1.255	1.254	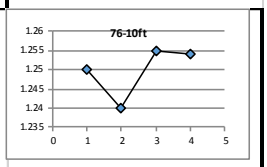
	//	28ft	496ft	1.25	1.21	1.202	1.318	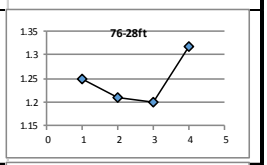
	END	**Joint**	518ft	1.21875	1.17	1.244	1.3	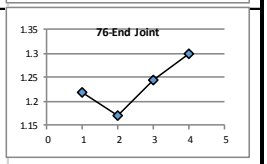
Total	11 pipes							

Figure B-11 Comparison of middle ordinate values (e) obtained at 45 degrees from MOP-119 method for all installation phases of pipe no.76

.

References

1. Abolmaali, A., Motahari, A., Hutcheson, J., & Le, T. “Evaluation of HDPE pipelines Structural Performace”, UT Arlington CSER 2010.
2. ACI 116R-00 Cement and Concrete Terminology, Reported by ACI committee 116.
3. ACI 229R-99 Controlled Low-Strength Materials, Reported by ACI committee 229.
4. American Society of Civil Engineers, “Steel Penstocks (MOP-79)”. ASCE Manual and Reports on Engineering Practice, 2012
5. American Water Works Association, 1997, Steel Water Pipe – 6in. and Larger, AWWA C200-97.
6. American Water Works Association, 2004, Steel pipe: a guide for design and installation, AWWA Manual 11, 4th Edition, Denver, CO.
7. American Water Works Association, C205-12 Cement–Mortar Protective Lining and Coating for Steel Water Pipe 4 In. (100 mm) and Larger. AWWA 2012
8. ASTM C31/C31M-12 Standard Practice for Making and Curing Concrete test Specimens in the Field, 2012
9. ASTM C78/C78M-10 Standard Test Method for Flexural Strength of Concrete (Using Simple Beam with Third-Point Loading), 2010
10. ASTM D 5971-07 Standard Practice for Sampling Freshly Mixed Controlled Low-Strength Material, 2007
11. ASTM D4832-10 Standard Test Method for Preparation and Testing of Controlled Low Strength Material (CLSM) Test Cylinders, 2010.
12. ASTM F1216-09 Standard Practice for Rehabilitation of Existing Pipelines and Conduits by the Inversion and Curing of a Resin-Impregnated Tube, 2009

13. Bellavar,F., “Large Diameter Steel Pipe Field Test Using Controlled Low Strength Material And Staged Construction Modelling Using 3-D Nonlinear Finite Element Analysis”, Thesis UTA 2013.
14. Boschert,J. & Butler,J. “CLSM as a Pipe Bedding: Computing Predicted Load using the Modified Marston Equation”, ASCE Pipelines 2013 conference.
15. Bosseler, B.H. & Stein, D., “Requirements for recording and analyzing deflection measurements in buried flexible pipes”, pp27-38, 1998.
16. Buried Flexible Steel Pipe, Design and Structural Analysis. American Society of Civil Engineers, 2009.
17. Dezfooli, M.S., “Staged Construction Modeling Of Large Diameter Steel Pipes Using 3-D Nonlinear Finite Element Analysis”, Dissertation UTA 2013.
18. Duran,O., & Seneviratne,D. “Pipe Inspection Using a Laser-Based Transducer and Automated Analysis Techniques”, IEEE 2003.
19. Howard, A. “The Reclamation E’ Table, 25 years Later”, presented at Plastics Pipe XIII International Conference, 2006
20. Jeyapalan, Jey K., “Advances in underground pipeline design, construction and management”, 2007.
21. Moser, A. P., “Buried pipe design”, New York: McGraw-Hill, 2001.
22. Pipeline and Drainage Consultants, “Evaluation of HDPE Pipe Performance on Kentucky DOT and Ohio Dot Construction Projects”, ACPA 2006.
23. Sharma, J.R., Najafi, M., Marshall, D., & Jain, A. “Thin-walled Large Diameter Steel Pipe Response to Various Embedment Conditions”, Pipelines ASCE 2013.
24. Simmons, A.R. “Use of Flowable Fill as Backfill Material Around Buried Pipes”, 2002.
25. Smith, A. “Controlled low strength material”, The Aberdeen group 1991

26. Zhao, J., Kuraocka, S., Baker, T., Gu, P., Brousseau, S., & Brousseau, R., “Durability and Performance of Gravity Pipes: A State-of-the-Art Literature Review” IRC, 1998.

Biographical Information

Saman F Gozarchi was born in Babol,Iran and grew up in Gaborone,Botswana. In the Fall of 2009, he moved to the United States to pursue a higher education and in May of 2012 obtained a Bachelor of Science in Civil engineering at the University of Texas at Arlington (UTA). In the fall of 2012, he extended his studies by enrolling in the Master's program (Structural Engineering) at UTA, and in 2013, he had the wonderful opportunity to work as a Graduate Research assistant with Dr. Ali Abolmaali. At the time of the completion of this thesis, Saman plans to obtain professional licensure in civil engineering and work in industry before returning to school for a Doctoral degree (Ph.D.).